AN APPLICATION OF GRAPHICAL MODELS TO FMRI DATA

USING THE LASSO PENALTY

by

THADDEUS ROBERT SULEK

(Under the Direction of Cheolwoo Park)

ABSTRACT

In this thesis, we study the graphical lasso method and apply it to functional magnetic resonance imaging (fMRI) data. The graphical lasso method enables one to construct undirected sparse graphs between variables of interest. The fMRI data concerns subjects' brain activities while they engage in saccadic eye movement tasks. The datasets are collected before and after they practice certain tasks. Using the graphical lasso procedure, we create undirected graphs that display the connections between the different regions of interest (ROI) in the brain. By controlling the regularization parameter in this lasso procedure, we identify which ROIs are more strongly connected than the others. We compare these undirected graphs before and after the practice and also across different practice groups.

INDEX WORDS: Functional Magnetic Resonance Imaging Data, Graphical Model, Lasso, Regions of Interest

AN APPLICATION OF GRAPHICAL MODELS TO FMRI DATA USING THE LASSO PENALTY

by

THADDEUS ROBERT SULEK

Bachelor of Arts, Coker College, 2013

Masters of Science, College of Charleston, 2015

A Thesis Submitted to the Graduate Faculty of The University of Georgia in Partial Fulfillment of the Requirements for the Degree

MASTER OF SCIENCE

ATHENS, GEORGIA

2017

AN APPLICATION OF GRAPHICAL MODELS TO FMRI DATA

USING THE LASSO PENALTY

by

THADDEUS ROBERT SULEK

Major Professor:	Cheolwoo Park
Committee:	Nicole Lazar
	Jennifer McDowell

Electronic Version Approved:

Suzanne Barbour
Dean of the Graduate School
The University of Georgia
May 2017

DEDICATION

To my parents (Bob and Nancy), brothers (Josh and Noah), sisters (Maggie and Anna), several special friends and my beloved Lauren

SPECIAL DEDICATION

In loving memory of my grandmother Joan Traina

ACKNOWLEDGEMENTS

I would like start by thanking the faculty at the University of Georgia for preparing me for life after school and all of the lessons I have learned from working with them throughout these last couple years. I would especially like to thank Dr. Cheolwoo Park for taking a chance on me and accepting me into the phenomenal statistics department at UGA so I could pursue a degree in higher education. He has been my teacher in classes, mentored me throughout my thesis and motivated me to reach all the goals I had when I arrived at UGA. I am extremely thankful for his boundless patience with me and his support that extends past the role he held as my advisor and professor.

Furthermore, I would like to thank my committee members, Dr. Nicole Lazar and Dr. Jennifer McDowell for their recommendations and careful reading. I am also thankful for my fellow statistics graduate students contributions to my work this year and making these last couple years a fantastic experience for me. Without their support this work would not have been possible. I would also like to thank my love, Lauren, and her family for their unconditional love and motivation throughout this process. Last but not least, I would like to thank my family for their long-term support and endless love. I am grateful for all the sacrifices they have made to allow me to pursue my dreams and receive a great education.

TABLE OF CONTENTS

Page

ACKNOWLEDGEMENTS ..... #v

LIST OF TABLES ..... #viii

LIST OF FIGURES ..... #ix

CHAPTER

1 INTRODUCTION ..... #1

1.1 BACKGROUND ..... #1

2 LITERATURE REVIEW ..... #3

2.1 THE LASSO PROCEDURE ..... #3

2.2 PENALIZED GAUSSIAN LOG-LIKELIHOOD FUNCTIONS ..... #4

2.3 COORDINATE DESCENT ALGORITHMS ..... #5

3 DATA ..... #7

3.1 THE EXPERIMENTS ..... #7

3.2 DATASET REVIEW AND REGIONS OF INTEREST ..... #8

4 PROCESS ..... #10

4.1 IMPLEMENTATION ..... #10

4.2 GRAPH ESTIMATION PIPELINE ..... #11

4.3 UNDIRECTED GRAPH ..... #12

4.4 EXAMPLE ..... #14

4.5 HEAT GRAPH ..... #16

5 RESULTS .....#20

5.1 DATASET COMPARISONS .....#20

5.2 OVERALL RESULTS .....#29

5.3 INDIVIDUAL TEST RESULTS .....#31

6 CONCLUSION .....#41

REFERENCES .....#42

LIST OF TABLES

Page

Table 3.1: ROI Overview.....#8

Table 5.1: General practice group for 0% event.....#21

Table 5.2: Specific practice group for 0% event.....#22

Table 5.3: General practice group for 100% event.....#23

Table 5.4: Specific practice group for 100% event.....#24

Table 5.5: General practice group for 50% event.....#25

Table 5.6: Specific practice group for 50% event.....#26

Table 5.7: General practice group for blocked-design.....#27

Table 5.8: Specific practice group for blocked-design.....#28

Table 5.9: Most Frequent Connections.....#30

Table 5.10: Most Frequent Connections by Group.....#31

Table 5.11: General practice group at pre-test for blocked-design with subjects 1-2.....#33

Table 5.12: General practice group at pre-test for blocked-design with subjects 3-4.....#34

Table 5.13: General practice group at pre-test for blocked-design with subjects 5-6.....#35

Table 5.14: General practice group at pre-test for blocked-design with subjects 7-8.....#36

Table 5.15: General practice group at pre-test for blocked-design with subjects 9-10.....#37

Table 5.16: General practice group at pre-test for blocked-design with subjects 11-12.....#38

Table 5.17: General practice group at pre-test for blocked-design with subjects 13-14.....#39

Table 5.18: General practice group at pre-test for blocked-design with subjects 15-16.....#40

LIST OF FIGURES

Page

Figure 3.1: ROI Location .....#9

Figure 4.1: HUGE pipeline .....#12

Figure 4.2: Undirected Graph with Lambda value = 0.92 .....#13

Figure 4.3: Undirected Graph with Lambda value = 0.91 .....#13

Figure 4.4: Example of an Undirected Graph .....#15

Figure 4.5: Heat Graph in R Studio .....#17

Figure 4.6: Heat Graph Zoomed In .....#18

Figure 4.7: Manipulate Lever .....#18

Figure 4.8: Heat Graphs with Lambda values equal to 0.91 and 0.92 .....#19

Figure 5.1: General practice group at pre-test (Left) and post-test (Right) for 0% event.....#21

Figure 5.2: Specific practice group at pre-test (Left) and post-test (Right) for 0% event .....#22

Figure 5.3: General practice group at pre-test (Left) and post-test (Right) for 100% event.....#23

Figure 5.4: Specific practice group at pre-test (Left) and post-test (Right) for 100% event .....#24

Figure 5.5: General practice group at pre-test (Left) and post-test (Right) for 50% event.....#25

Figure 5.6: Specific practice group at pre-test (Left) and post-test (Right) for 50% event .....#26

Figure 5.7: General practice group at pre-test (Left) and post-test (Right) for blocked-design ..#27

Figure 5.8: Specific practice group at pre-test (Left) and post-test (Right) for blocked-design..#28

Figure 5.9: General practice group at pre-test for blocked-design with subjects 1-2 .....#33

Figure 5.10: General practice group at pre-test for blocked-design with subjects 3-4 .....#34

Figure 5.11: General practice group at pre-test for blocked-design with subjects 5-6 .....#35

Figure 5.12: General practice group at pre-test for blocked-design with subjects 7-8 .....#36

Figure 5.13: General practice group at pre-test for blocked-design with subjects 9-10 .....#37

Figure 5.14: General practice group at pre-test for blocked-design with subjects 11-12 .....#38

Figure 5.15: General practice group at pre-test for blocked-design with subjects 13-14 .....#39

Figure 5.16: General practice group at pre-test for blocked-design with subjects 15-16 .....#40

CHAPTER 1

INTRODUCTION

1.1 BACKGROUND

Graphical models are a tool implemented to simplify complicated systems and to describe the relationship among multiple random variables. These models use a graph-based representation as the basis for compactly encoding a complex distribution over a high-dimensional space (Koller and Friedman, 2012). They are frequently performed in machine learning, probability theory and statistics. Another area that graphical models are implemented in is functional magnetic resonance imaging (fMRI) data.

One way to examine human brain activity is through the use of the fMRI procedure. FMRI data are generated by computing the variations in blood flow throughout different regions (or voxels) of the brain by means of Blood-Oxygen-Level-Dependent (BOLD) contrast. This type of high-dimensional data presents many "big data" problems regarding the construction of the brain network. Traditional methods for this type of analysis might not apply to datasets of this magnitude, so many new statistical methods are being developed. According to Luo (2014), a significant scientific question is how these brain areas are associated, which is termed brain connectivity. This brings us to the goal of this thesis, which is to apply graphical models to fMRI data for the purpose of finding the connections between different regions of the brain.

In this thesis, we offer an interpretable technique for brain network estimation from fMRI data. In Chapter 2, we review related statistical methods such as: the lasso method, penalized

Gaussian log-likelihood estimation, coordinate descent algorithm, and graph estimation. Then we introduce the motivating dataset and how it was extracted in Chapter 3. In Chapter 4, we focus on the techniques used to evaluate the dataset and the results from the analysis. In Chapter 5, we highlight the different regions of the brain that boast the strongest connections detected from the fMRI data. Finally, we conclude by discussing potential future work in this field.

CHAPTER 2

LITERATURE REVIEW

2.1 THE LASSO PROCEDURE

Recently many statisticians have suggested the L_1 (lasso) penalty for the estimation of sparse undirected graphical models. LASSO (least absolute shrinkage and selection operator) is a regression analysis method that performs variable selection and regularization. In this context, regularization is a procedure of preventing over-fitting and is controlled by the regularization parameter, – λ. This method enhances the accuracy and interpretability of the model it produces. The lasso method improves prediction error by shrinking large regression coefficients, reducing overfitting, and forcing small coefficients to be exactly zero.

Tibshirani (1996) defines the lasso method in (2.1.1) with the data $(\mathbf{x}_i, y_i)$, $i = 1, 2, \cdots, N$, where $\mathbf{x}_i = \left(x_{i1}, \cdots, x_{ip}\right)^T$ are the predictor variables and y_i are the response variables. In this situation, we assume the observations are independent or the responses are conditionally independent given the predictor variables. We must also assume the x_{ij} are standardized. Then if we let $\hat{\beta} = \left(\hat{\beta}_1, \cdots, \hat{\beta}_p\right)^T$, the lasso estimate $\left(\hat{\alpha}, \hat{\beta}\right)$ is defined by

$$\left(\hat{\alpha}, \hat{\beta}\right) = \operatorname{argmin}\left\{\sum_{i=1}^{n}\left(y_i - \alpha - \sum_j \beta_j x_{ij}\right)^2\right\} \text{ subject to } \sum_j \left|\beta_j\right| \leq \lambda. \qquad (2.1.1)$$

In (2.1.1), $\lambda \geq 0$ and it controls the shrinkage that is applied to the estimates. As $\lambda \to 0$, it forces the sum of the absolute value of the regression coefficients to be less than a fixed value and it

essentially chooses a simpler model with fewer coefficients. For any value of λ, the result for α is $\hat{\alpha} = \bar{y}$ and without loss of generality we assume $\bar{y} = 0$, so it is reasonable to remove α from (2.1.1).

2.2 PENALIZED GAUSSIAN LOG-LIKIHOOD FUNCTIONS

As of late, substantial development has been made on designing efficient algorithms to learn sparse undirected graphs from high-dimensional datasets. The majority of these approaches are constructed from penalized maximum-likelihood estimation. The penalized Gaussian log-likelihood functions are used in this thesis for variable selection and parameter estimation. They originated from the multivariate Gaussian log-likelihood function:

$$\ln p(X|\mu, \Sigma) = -\frac{n}{2}\log|\Sigma| - \frac{1}{2}\left(\sum_{i=1}^{n}(x_i - \mu)'\Omega(x_i - \mu)\right) + c.$$

Here there are n multivariate normal observations, $(x_1, \cdots, x_n)$, with p dimensions, mean μ, covariance $\sum$, inverse covariance matrix $\sum^{-1} = \Omega$, and constant term c.

Meinshausen and Bühlmann (2006) take a simple approach to sparse graphical model estimation by fitting a lasso model to each variable and using the remaining variables as predictors. Yuan and Lin (2007) suggest a more complicated approach to achieve a sparse graph structure and to give a better estimator of the concentration matrix Ω. They adapt the L_1 (lasso) penalty (Tibshirani, 1996) and seek the minimizer $\left(\hat{\mu}, \hat{\Omega}\right)$ of

$$-\log|\Omega| + \frac{1}{n}\sum_{i=1}^{n}(x_i - \mu)'\Omega(x_i - \mu) \text{ subject to } \sum_{i \neq j}\left|\Omega_{ij}\right| \leq \lambda, \tag{2.2.1}$$

where λ represents the tuning parameter. Since we are assuming the x_i are standardized, we can re-write (2.2.1) as

$$-\log|\Omega| + \frac{1}{n}\sum_{i=1}^{n} x_i\,'\Omega x_i \text{ subject to } \sum_{i\neq j}|\Omega_{ij}| \leq \lambda.$$

This can further be re-written as

$$-\log|\Omega| + \text{tr}(S\Omega) \text{ subject to } \sum_{i\neq j}|\Omega_{ij}| \leq \lambda,$$

where S represents the empirical covariance matrix and $\text{tr}(S\Omega)$ represents the trace of $S\Omega$. Yuan and Lin (2007) also clarify that since the objective function and feasible region of the previous equation are convex, we can equivalently use the Langrangian form

$$-\log|\Omega| + \text{tr}(S\Omega) + \lambda\sum_{i\neq j}|\Omega_{ij}|.$$

To determine conditional independence between the p variables, we must examine Ω. A nonzero off-diagonal entry in Ω means the matching i^{th} and j^{th} variables are directly connected. Likewise, a zero in the off-diagonal implies the i^{th} and j^{th} variables are conditionally independent, given all other variables and there is no connection between them.

2.3 COORDINATE DESCENT ALGORITHMS

The convex optimization problems mentioned in the previous section can be solved using coordinate descent (CD) algorithms by sequentially executing rough minimization along coordinate directions or coordinate hyperplanes. Wright (2015) mentions that CD methods are the archetype of an almost universal approach to algorithmic optimization: solving an optimization problem by solving a sequence of simpler optimization problems. It is a one-at-a-time update scheme, where each iterate is attained by fixing the majority of the variable vector x at their present iteration, and approximately minimizing the objective with respect to the

remaining components. The remaining lower dimensional problems are normally more easily solved than the full problem.

In the graph estimation that we conduct, we apply CD with active set and covariance update to minimize the penalized Gaussian log-likelihood functions. This will rotate through all of the variables and fit a modified lasso regression to each variable in turn. These individual lasso problems are then solved by CD.

CHAPTER 3

DATA

3.1 THE EXPERIMENTS

In this thesis, we apply graphical models to datasets from an experiment that investigated low and high levels of cognitive control through ocular motor circuitry underlying saccade production. Cognitive control refers to the development of planning and goals to effect behavior and saccade refers to a swift movement of the eye between fixation points. The purpose of this experiment was to determine if practice and familiarity to the saccade trials would decrease the cognitive control that would be needed to trigger the appropriate task set.

The dataset came from an experiment conducted on young healthy adults and only included two types of trials: prosaccade trials of looking toward a stimulus and antisaccade trials of looking to the mirror image. Pierce and McDowell (2017) set up the experiment so these two trials were presented in five mixed runs with varying probability of antisaccade to prosaccade trials (0%, 25%, 50%, 75%, or 100%) and the data was recorded at 158 time points (or volumes). In addition to these five runs there was also a blocked-design run that presented alternating blocks of antisaccade and prosaccade tasks, and the data was logged at 170 time points. They split up the participants into two groups following the pre-test (before any exposure to practice tests), one group practiced only antisaccade trials (the "general" group), while the other group practiced the same five runs of differing probabilities as they performed in the initial test (the "specific" group). After four days of practice, a posttest fMRI session was conducted to

compare the results and determine if less cognitive control was needed to perform the tasks. Pierce and McDowell (2017) hypothesized that the cognitive control regions associated with these tasks, like the prefrontal cortex and anterior cingulate cortex, would show a decrease in BOLD activation at posttest.

3.2 REVIEW DATASETS AND REGIONS OF INTEREST

The dataset had 32 participants (split into two practice sets of 16), included 37 of 38 (40 × 48 voxels in size) slices of the brain, and had 158 volumes for the 0-100% events and 170 for the block design event. When this experiment was conducted, the datasets were centered around different areas of the brain, which we will refer to as 'regions of interest' or ROI. This dataset includes twenty of these ROI and each of them is listed in Table 3.1 below.

Table 3.1: ROI Overview

Region of Interest	**Abbreviation**	**Left and Right**
Prefrontal Cortex	PFC	Both
Supplementary Eye Field	SEF	Neither
Medial Frontal Eye Field	mFEF	Both
Lateral Frontal Eye Field	lFEF	Both
Inferior Frontal Cortex	IFC	Left
Thalamus	Thal	Both
Basal Ganglia	BG	Both
Inferior Parietal Lobule	IPL	Both
Precuneus	Precun	Both
Middle Occipital Gyrus	MOG	Both
Cuneus	Cun	Both

Remark. These ROIs were the columns of the datasets and the time points were the rows. Each ROI is one time series averaged over subjects and voxels in that area (ROI).

It is also important to note the approximate location of these ROIs in the brain. Figure 3.1 displays the ROI in positional order. The blue circles are the frontal, orange are the

subcortical, red are the parietal, and green are the occipital. This structure will be used later, to display the connections between the ROIs.

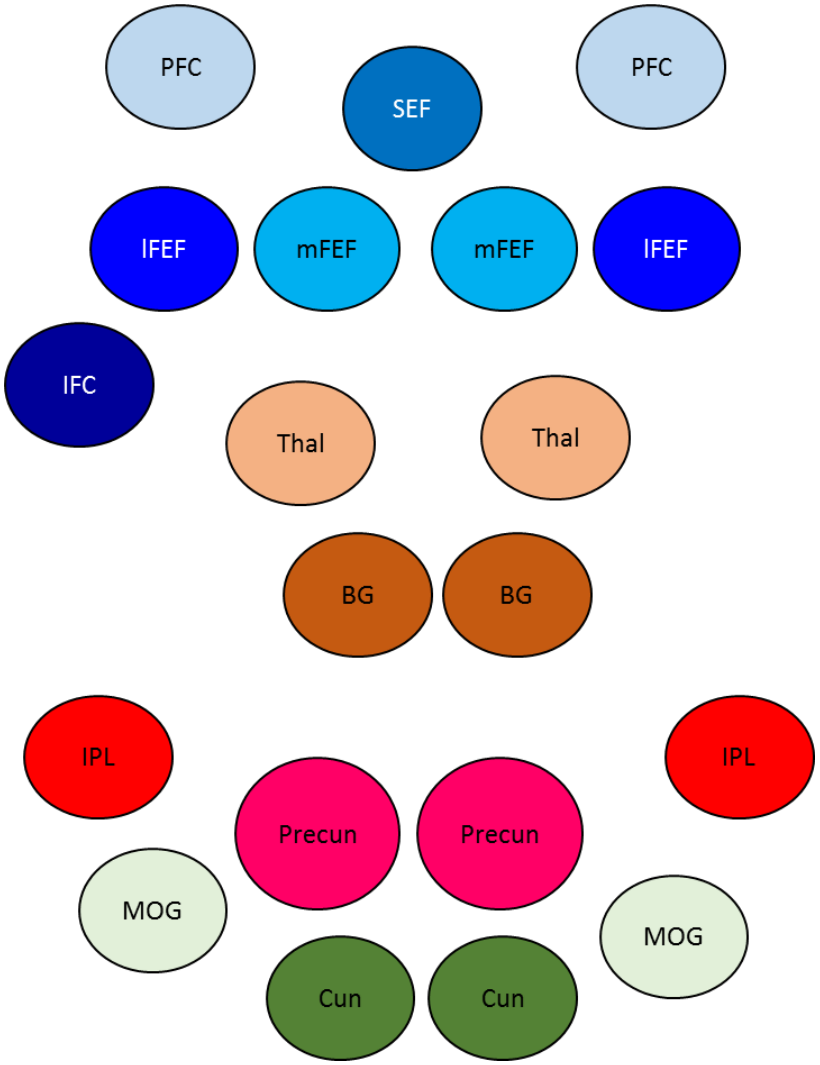

Figure 3.1: ROI Location

CHAPTER 4

PROCESS

4.1 IMPLEMENTATION

The computer programming language R was used in this thesis to apply graphical models to the fMRI datasets. The R packages that were implemented include the following: HUGE, glasso, manipulate, igraph, and fields. To create visualizations of the fMRI data we use an R package called HUGE (high dimensional undirected graphs). This package allows the user to input either the covariance matrix or the data matrix into it, and it detects which matrix it is by the symmetry of it. The code is also memory-optimized using sparse matrix data structures so that it can handle larger datasets when estimating and storing full regularization paths (Zhao et al., 2012). It provides an additional graph estimation method based on thresholding the sample correlation matrix. We take a closer look at this package in Section 4.2, when we examine the graph estimation pipeline.

The other packages also helped create the visualizations. The glasso package is used to estimate the sparse inverse covariance matrix using a lasso (ℓ_1) penalty. The manipulate package is used to create an interactive plot that featured a lever allowing the user to adjust the regularization parameter for the lasso method. As the lever changes, so does the plot. The igraph package is used to implement graph algorithms (like the graphical lasso algorithm) and handles large graphs with ease. The fields package is used to implement sparse matrix methods for our large dataset.

4.2 GRAPH ESTIMATION PIPELINE

To describe the conditional independence among variables in the fMRI data, we use heat and undirected graphs created through the `HUGE` package in `R`. This package offers several different modules, but only a few of them were used in this project and they can be seen below in Figure 4.1. To start, there is a data generator that can generate multivariate Gaussian data, but we are using data from an experiment so we did not need to use this module. The next module is a screening process of either the lossless screening or lossy screening. Zhao et al. (2012) mention that this part of the pipeline is meant to control the use of large-scale correlation screening prior to graph estimation and these screening methods can dramatically decrease the computational rate. They can also demonstrate equal or better estimation by reducing the variance; however it is at the cost of a slight increase in bias.

Following inputting the data and screening process comes graph estimation and this package offers two types: the covariance selection algorithm (Meinshausen and Bühlmann, 2006) and the graphical lasso algorithm (Friedman et al., 2010b). In this project we implement the latter of the two. This package also provides three regularization parameter selection methods: the stability approach for regularization selection, a modified rotation information criterion, and the extended Bayesian information criterion. The extended Bayesian information criterion is the only one applicable for the graphical lasso method and it is a log-likelihood model based selection criterion (Zhao et al., 2012). Lastly, there is a visualization of these estimated graphs and paths through the `igraph` package, where we are able to create undirected and heat graphs.

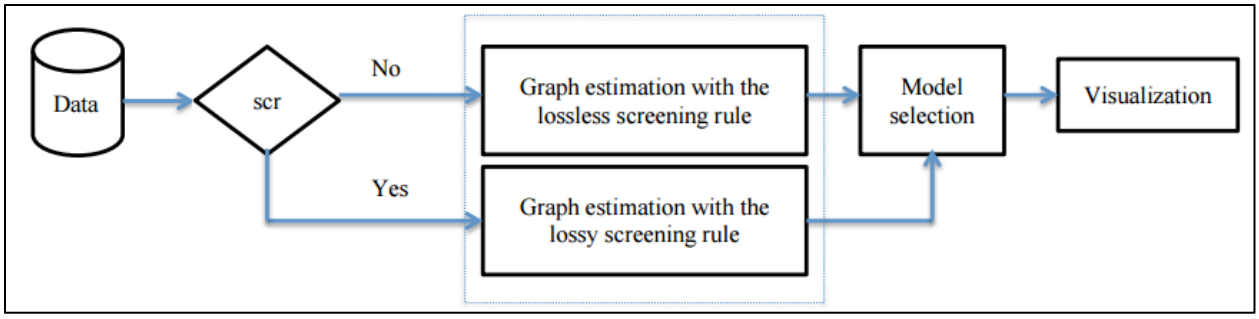

Figure 4.1 HUGE pipeline

4.3 UNDIRECTED GRAPH

Undirected graphs are a natural approach to describe the conditional independence among many variables. Each node of the graph represents a single variable (a region of interest in the brain) and no edge between two variables implies that they are conditional independent given all other variables. It is called an undirected graph because each edge is bi-directional, opposed to a directed graph where each edge points to a node. In the past decade significant progress has been made on designing efficient algorithms to learn undirected graphs from high-dimensional observational datasets (Zhao et al., 2012). The majority of these methods are based on the penalized maximum-likelihood estimation that we discussed in Section 2.2.

Figures 4.2 and 4.3 are screen-shots of undirected graphs that were created in this thesis. As clearly shown in the figures, there are twenty nodes that are each labeled by the abbreviation for the different ROI. The top part of the figures defines the λ value (regularization threshold) we are looking at. It is also important to note that these graphs represent three dimensional images, so the location of the nodes shifts in every frame when it is put into this two dimensional representation.

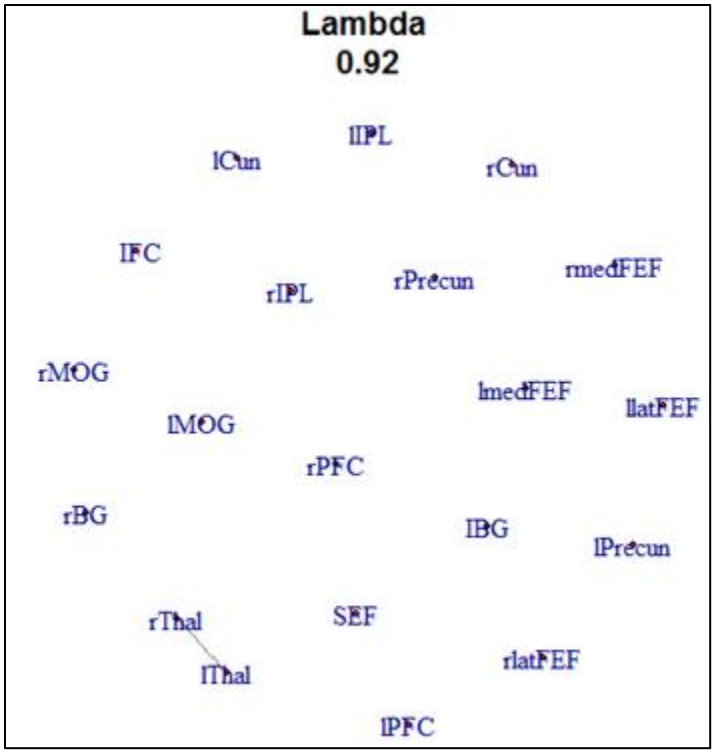

Figure 4.2 Undirected Graph with Lambda value = 0.92

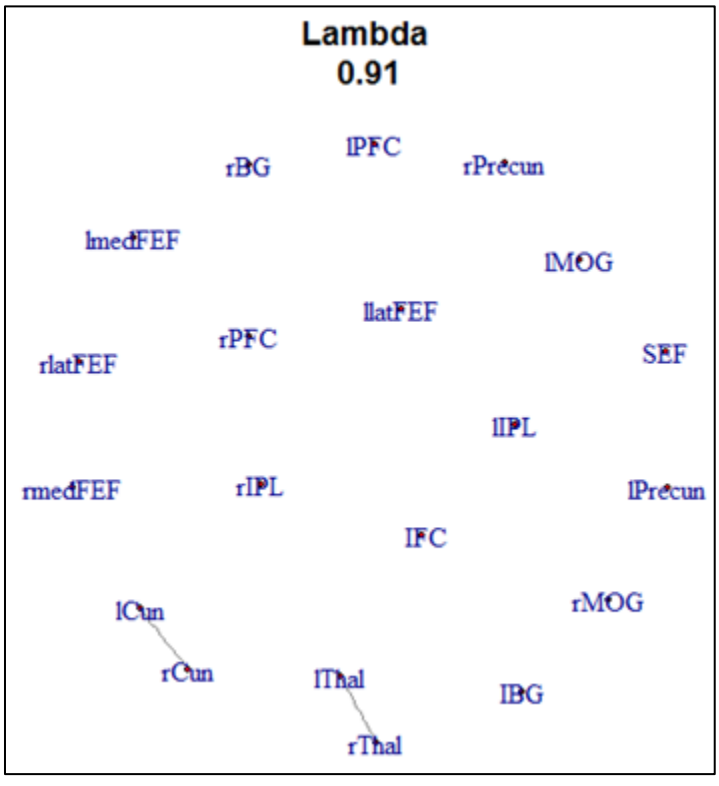

Figure 4.3 Undirected Graph with Lambda value = 0.91

In this case, Figure 4.2 has $\lambda = 0.92$ and one edge (connection) between the right thalamus and left thalamus. As λ decreases to 0.91 another edge gets added between the right cuneus and left cuneus. Given the setup of the algorithms used, the undirected graphs actually have stronger connections as λ increases. This value is less important to this study than the strength of the connections between the ROI.

4.4 EXAMPLE

Analyzing the fMRI data is a complicated task, so to better understand the behavior of the data; we will use an example with arbitrarily selected nodes instead of regions of the brain. Figure 4.4 displays this example in a step-by-step series of undirected graphs on how the data might behave as the lasso regularization parameter tightens. Progressing through each step, the weak connections between the covariates drop off first and the strongest are the last ones remaining. This example was created for the purpose of the viewer to see how the edges come in and out of the undirected graph. It is not intended to portray a relationship between any of these nodes.

The example begins, in step one, with the majority of the nodes connected to one another. In the second step the two edges, Grade – Intelligence and Grade – Happy, drop off. After a few more steps of different edges dropping off, we get to step five where the edge between Grade – Intelligence actually gets added back in. This is common to see in the fMRI data, and it happens because each step is independent of the other steps. This is similar to stepwise regression used for variable selection. As λ continues to decrease towards zero, more and more edges drop off until only the strongest connections remain. In the case of this example, Coherence and Difficulty have the strongest connection between one another.

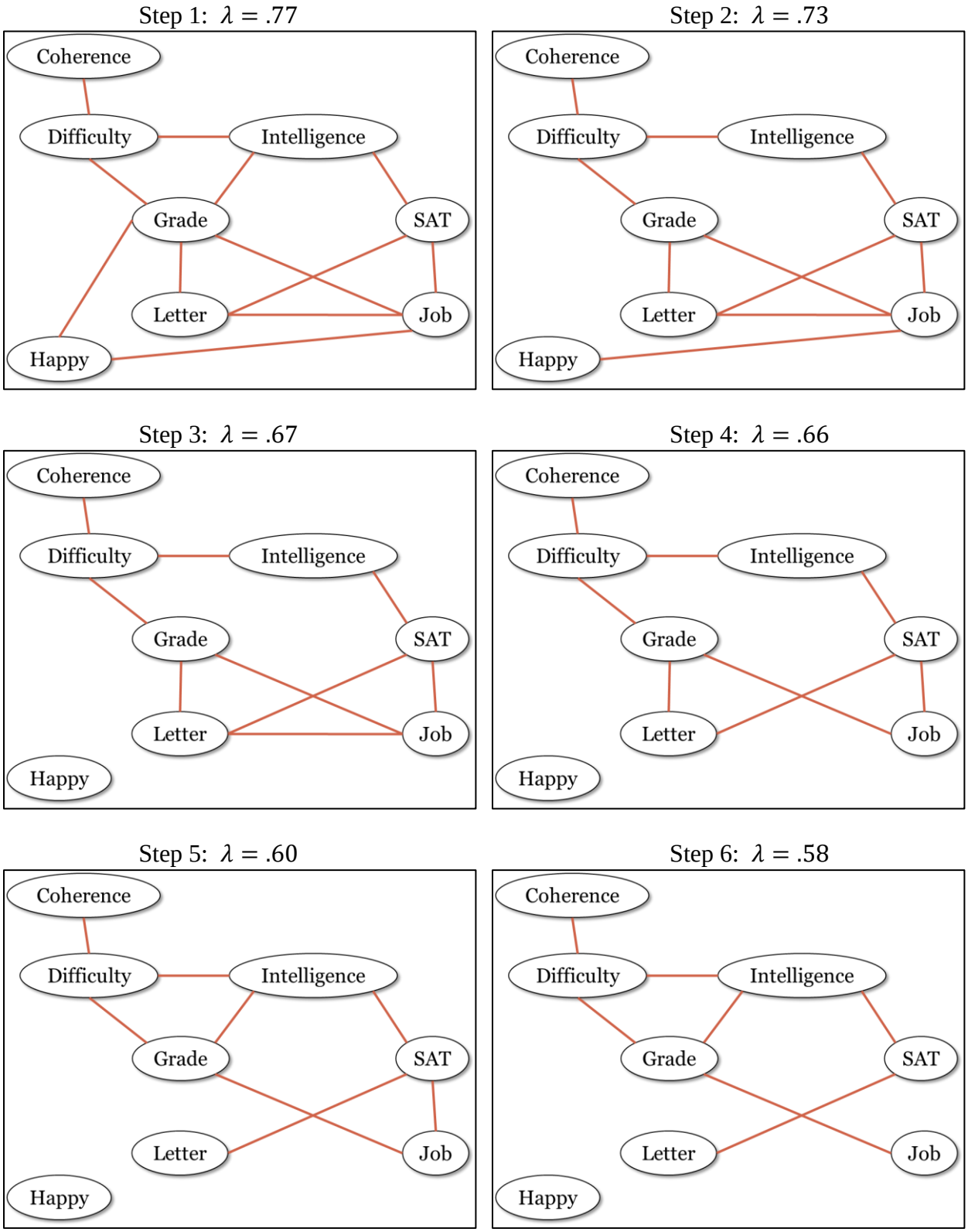

Figure 4.4 Example of an Undirected Graph

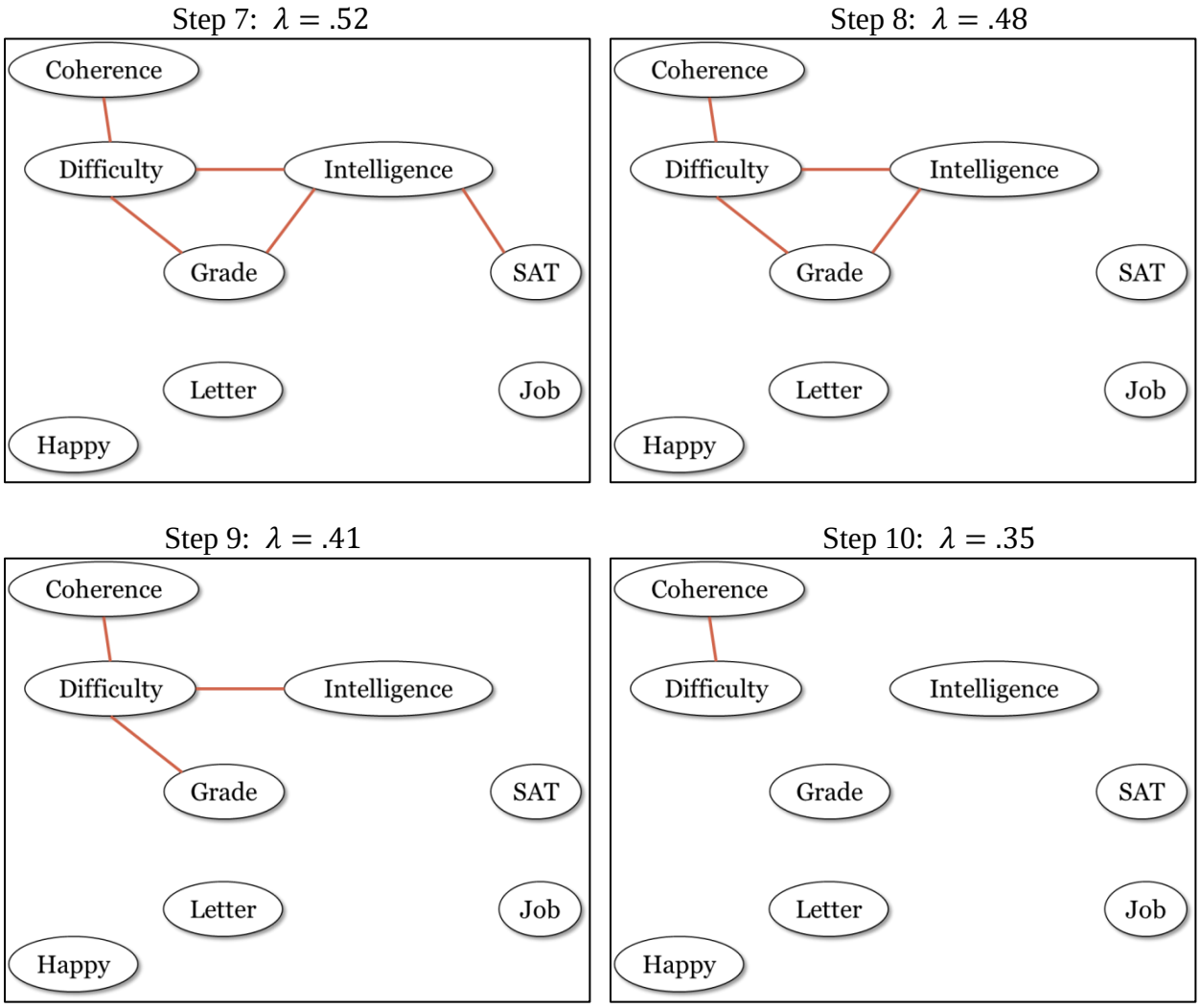

Figure 4.4 (Continued) Example of an Undirected Graph

4.5 HEAT GRAPH

In addition to undirected graphs, we were able to generate heat graphs to combat the always shifting undirected graphical images produced. The heat graphs offer a clearer view of the edges entering and exiting the model. Figure 4.5, is a screenshot of how the heat graph is portrayed in R studio with the manipulate lever used to control the tuning parameter. For a closer look at the manipulate lever view Figure 4.7.

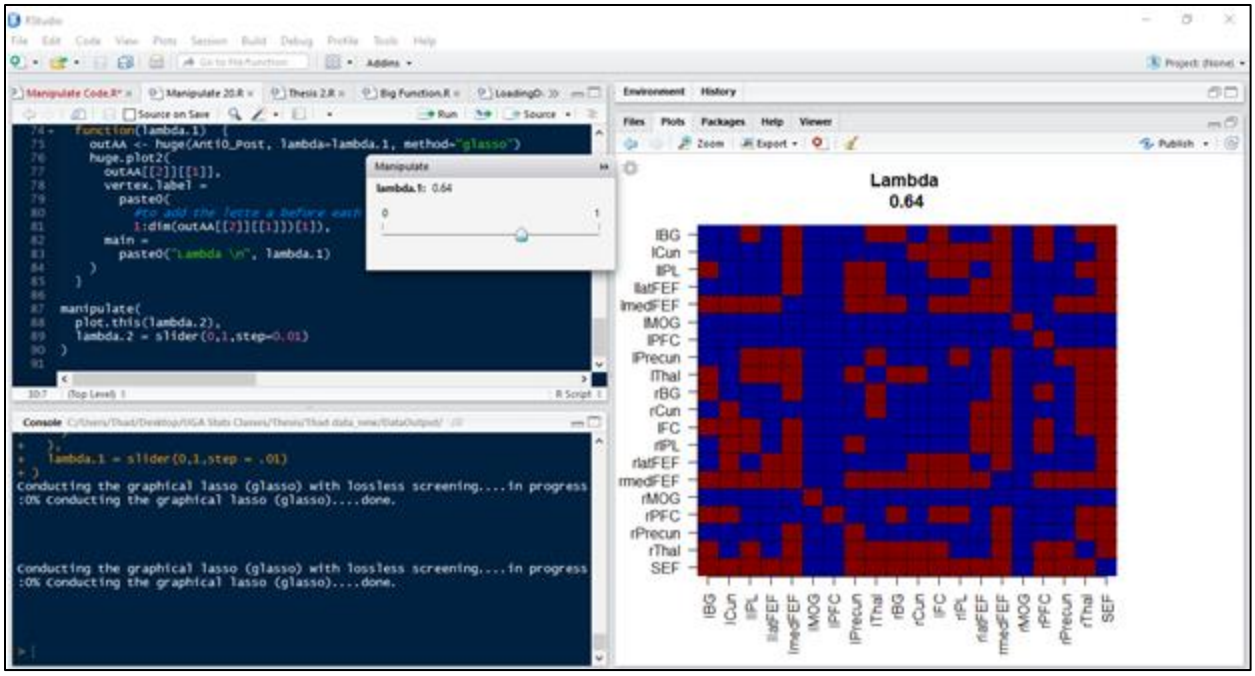

Figure 4.5 Heat Graph in R Studio

Figure 4.5 displays the R code used to create the heat graph on the upper left in the editor window, the console on the bottom left, and the heat graph in the plot on the right. Similar to the undirected graph, λ is centered above the graph and controlled through the manipulate lever in the center of the screen. This is a 20×20 graph with the abbreviations for each region of interest on the x and y axis's respectively. A red box indicates an edge and a blue box indicates no edge. Since this graph is symmetric each edge gets represented twice, so it is a bit easier to interpret the results when only half of it is observed. An image of the graph with half of it blocked out can be found below in Figure 4.6. There are also no edges connecting a node to itself, so the diagonal element of the graph will always be blue. Then to figure out which nodes are connected, one can trace each red block back to the x axis and y axis to find the nodes that are connected to one another.

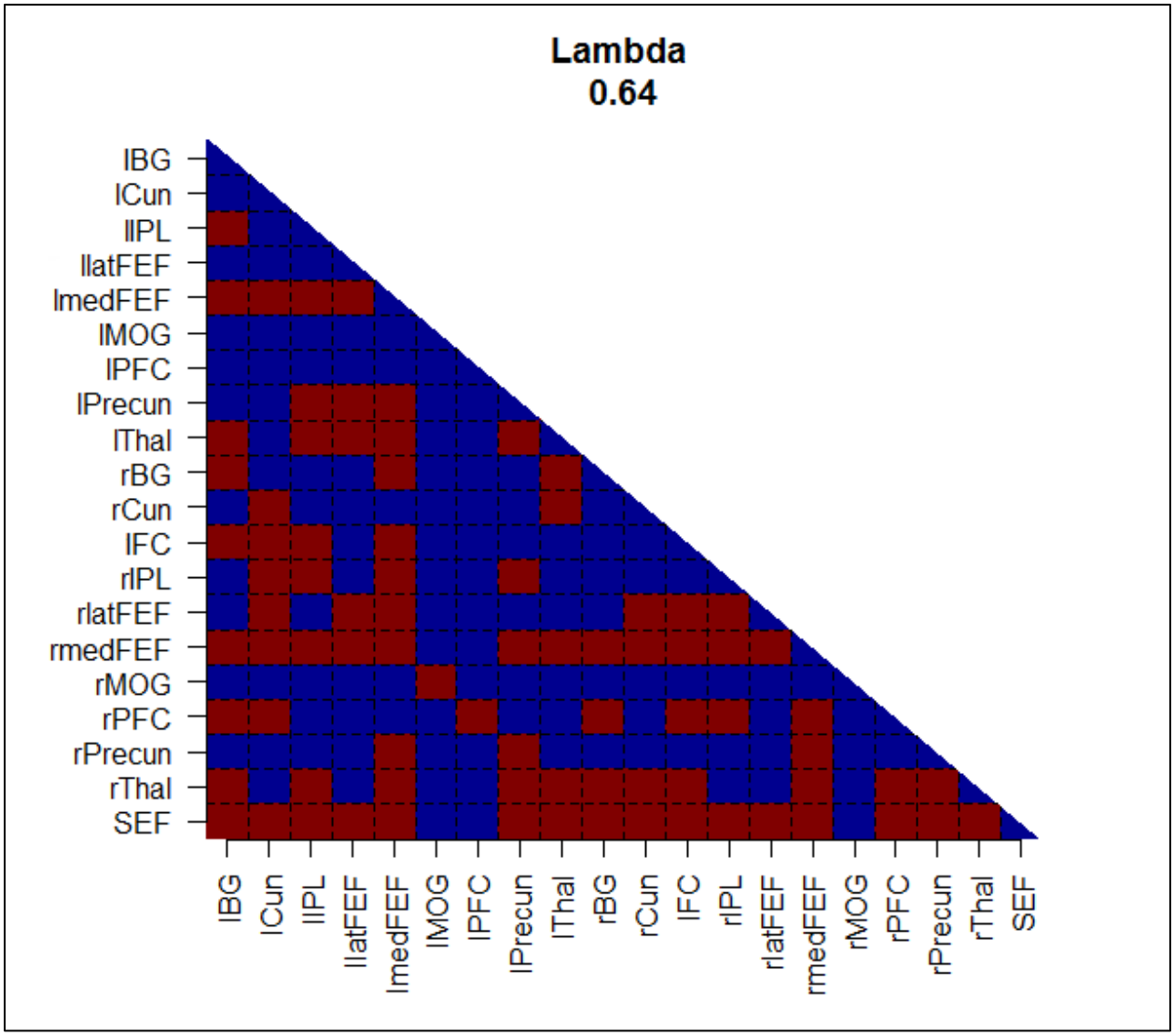

Figure 4.6 Heat Graph Zoomed In

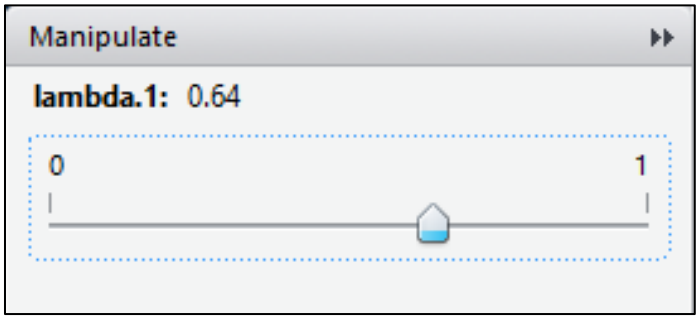

Figure 4.7 Manipulate Lever

Figure 4.8 displays the same demonstration used in the undirected graphs in Section 4.3. It is side-by-side heat graphs of fMRI data that has been shifted by $\lambda = 0.01$. When $\lambda = 0.91$, there are two connections between the left cuneus and the right cuneus and the right thalamus and left thalamus. The shift up has removed the edge between the left cuneus and right cuneus. This displays that the left thalamus and right thalamus have the strongest connection for this dataset. These heat graphs were used to carefully chart the edges exiting and entering each dataset. Again, if the symmetry of the graph is a distraction when recording the data, it is recommended to block out half the graph and only focus on one set of coordinates.

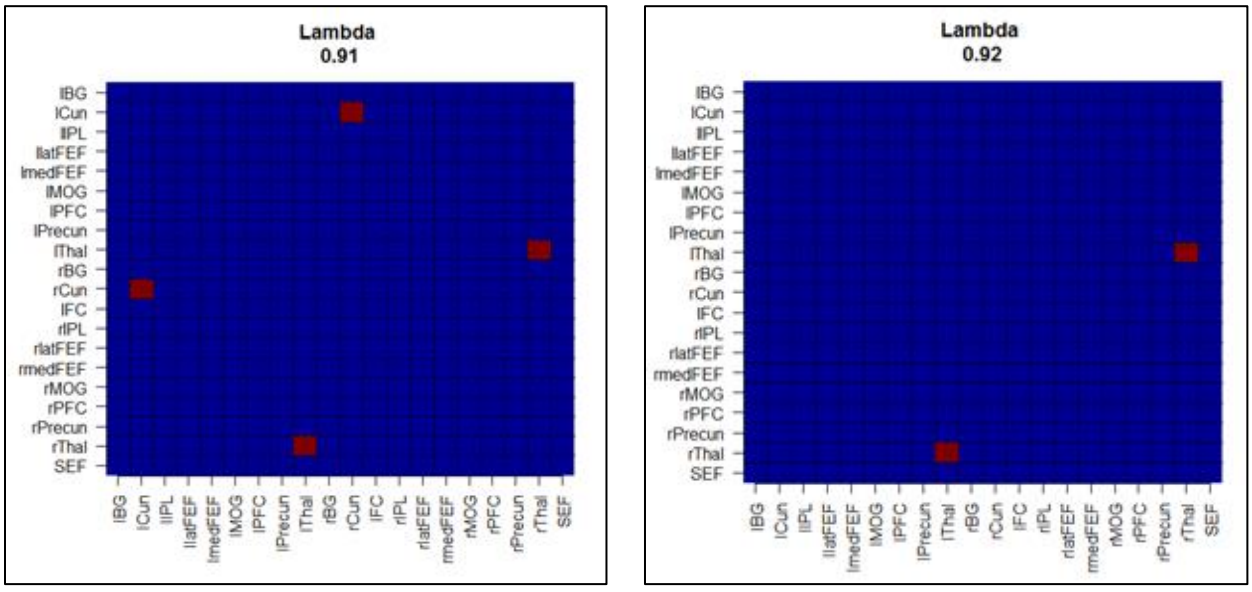

Figure 4.8 Heat Graphs with Lambda values equal to 0.91 and 0.92

CHAPTER 5

RESULTS

5.1 DATA COMPARISONS

After analyzing the graphical models for each dataset we can carefully compare and contrast the results to see if the cognitive control regions associated with these tasks showed any differences between groups and runs. To make these comparisons between the datasets we examined the ten strongest connections between the ROI and the order of their strength. The datasets that we wanted to closely compare were the 0% event with the 100% event and the 50% event and blocked-design. We also want to see how the "general" and "specific" practice groups compare to one another as well as the pre and post-test for each group. Recall that, for example, the 0% event includes no antisaccade trials and only features prosaccade trials.

We will display tables that indicate which group we are investigating, the strength of the connections, and the abbreviations for the ROI that are connected. Strength of connection will be on a scale of one to ten, with one being the strongest connection and ten being the weakest. Recall that some edges are removed from the model at the same time, so it is entirely possible that they have the same strength of connection. In the tables that follow, we have accounted for these connections that happen simultaneously and labeled them one after another, in an order that might match them up slightly better with their counter-part test for an easier comparison. These tables are followed by matching figures that give a visual of these ten strongest connections.

Table 5.1 General practice group for 0% event

Strength of Connection	ROI Connected	
	Pre-test	Post-test
1	lThal – rThal	lThal – rThal
2	lCun – rCun	lCun – rCun
3	lBG – rBG	lBG – rBG
4	rBG – rThal	rBG – rThal
5	lBG – lThal	lmedFEF – rmedFEF
6	lThal – rBG	lBG – lThal
7	lmedFEF – rmedFEF	lmedFEF – SEF
8	lmedFEF – lPrecun	lThal – rBG
9	lMOG – rMOG	lBG – rThal
10	lBG – rThal	lIPL – rmedFEF

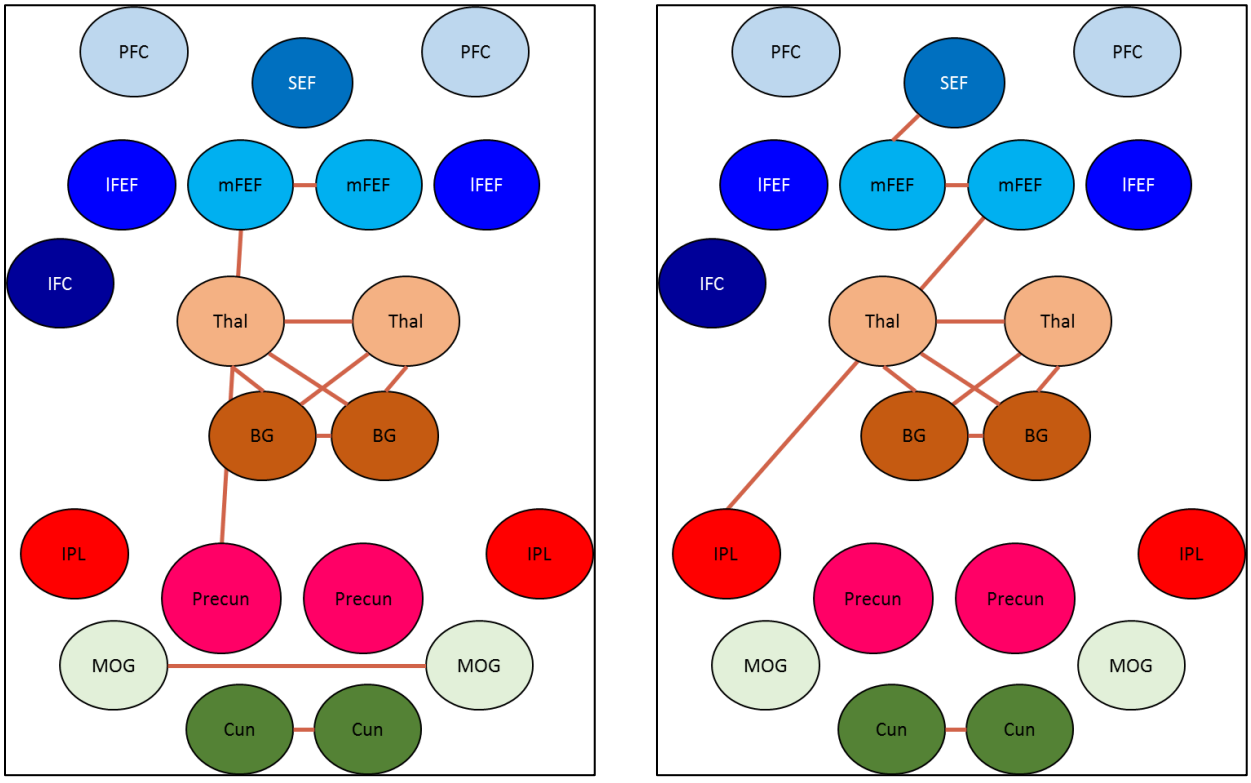

Figure 5.1 General practice group at pre-test (Left) and post-test (Right) for 0% event

Table 5.2 Specific practice group for 0% event

Strength of Connection	ROI connected	
	Pre-test	Post-test
1	lCun –rCun	lCun –rCun
2	lThal – rThal	lThal – rThal
3	lmedFEF – rmedFEF	lBG – rBG
4	lBG – rBG	rBG – rThal
5	lThal – rBG	lThal – rBG
6	rBG – rThal	lmedFEF – rmedFEF
7	rmedFEF – SEF	rmedFEF – SEF
8	lBG – lThal	lMOG – rMOG
9	lmedFEF – SEF	lmedFEF – SEF
10	llatFEF – rlatFEF	rPrecun – SEF

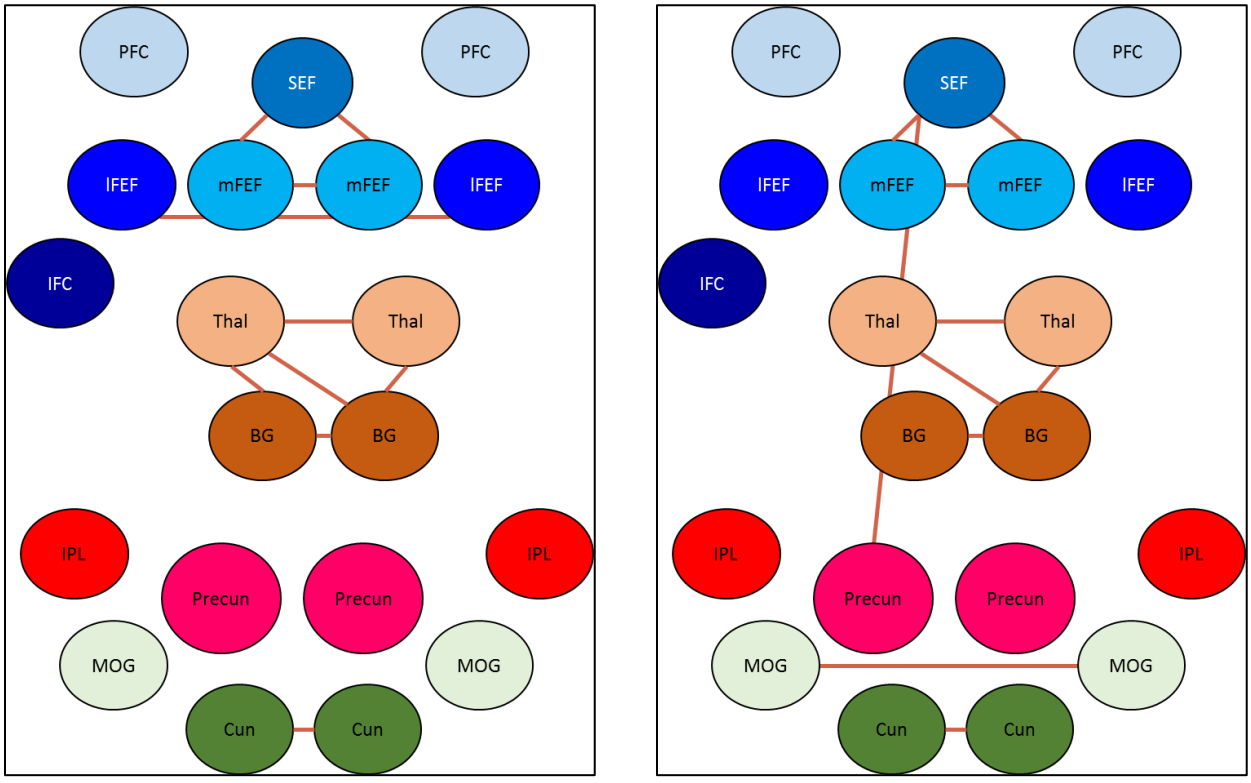

Figure 5.2 Specific practice group at pre-test (left) and post-test (Right) for 0% event (Left)

Table 5.3 General practice group for 100% event

Strength of Connection	ROI connected	
	Pre-test	Post-test
1	lCun – rCun	lCun – rCun
2	lmedFEF – rmedFEF	lmedFEF – rmedFEF
3	lBG – rBG	lThal – rThal
4	lThal – rThal	lBG – rBG
5	rBG – rThal	rBG – rThal
6	lBG – lThal	lBG – lThal
7	lThal – rBG	lThal – rBG
8	lmedFEF – lPrecun	lMOG – rMOG
9	lBG – rThal	rlatFEF – rmedFEF
10	lMOG - rMOG	rmedFEF - lCun

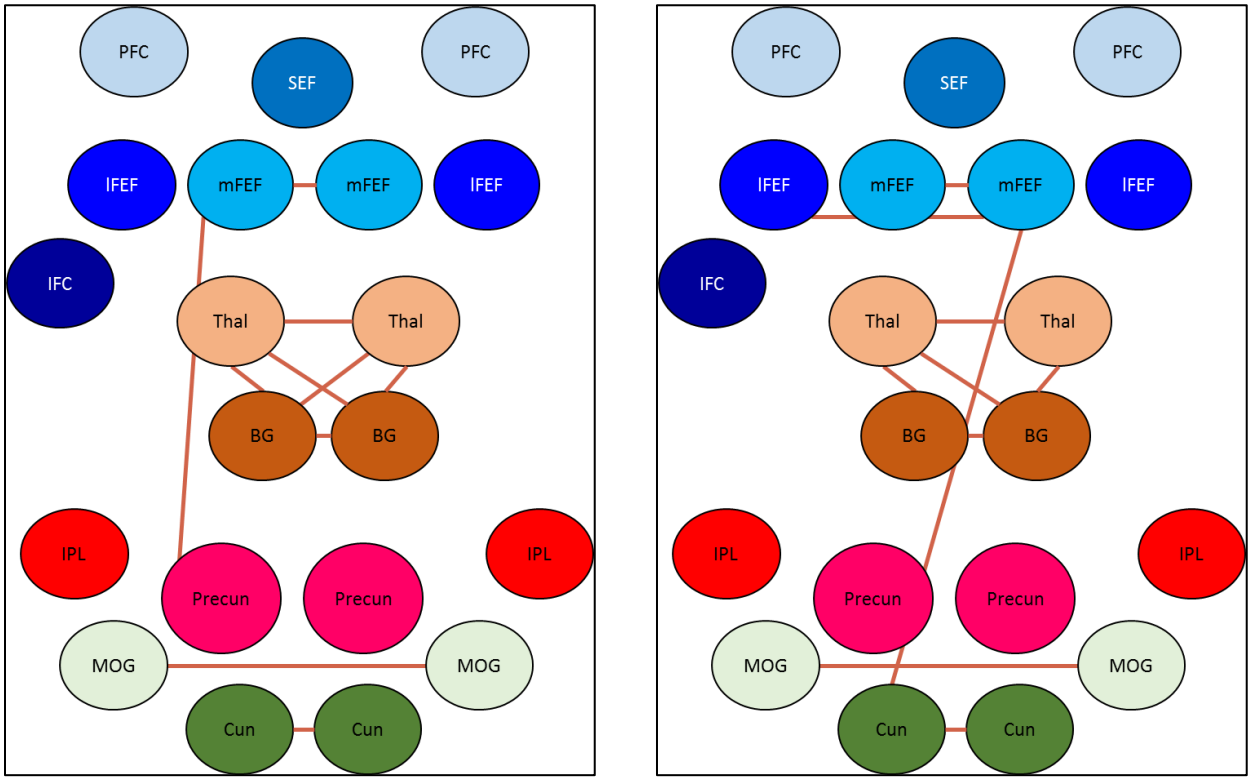

Figure 5.3 General practice group at pre-test (Left) and post-test (Right) for 100% event

Table 5.4 Specific practice group for 100% event

Strength of Connection	ROI connected	
	Pre-test	Post-test
1	lCun – rCun	lCun – rCun
2	lThal – rThal	lThal – rThal
3	lBG – rBG	lBG – rBG
4	lmedFEF – rmedFEF	lmedFEF – rmedFEF
5	rBG – rThal	lBG – lThal
6	lThal – rBG	rBG – rThal
7	lBG – lThal	llatFEF – lmedFEF
8	rmedFEF – SEF	lThal – rBG
9	lBG – rThal	llatFEF – SEF
10	lmedFEF – SEF	rmedFEF – SEF

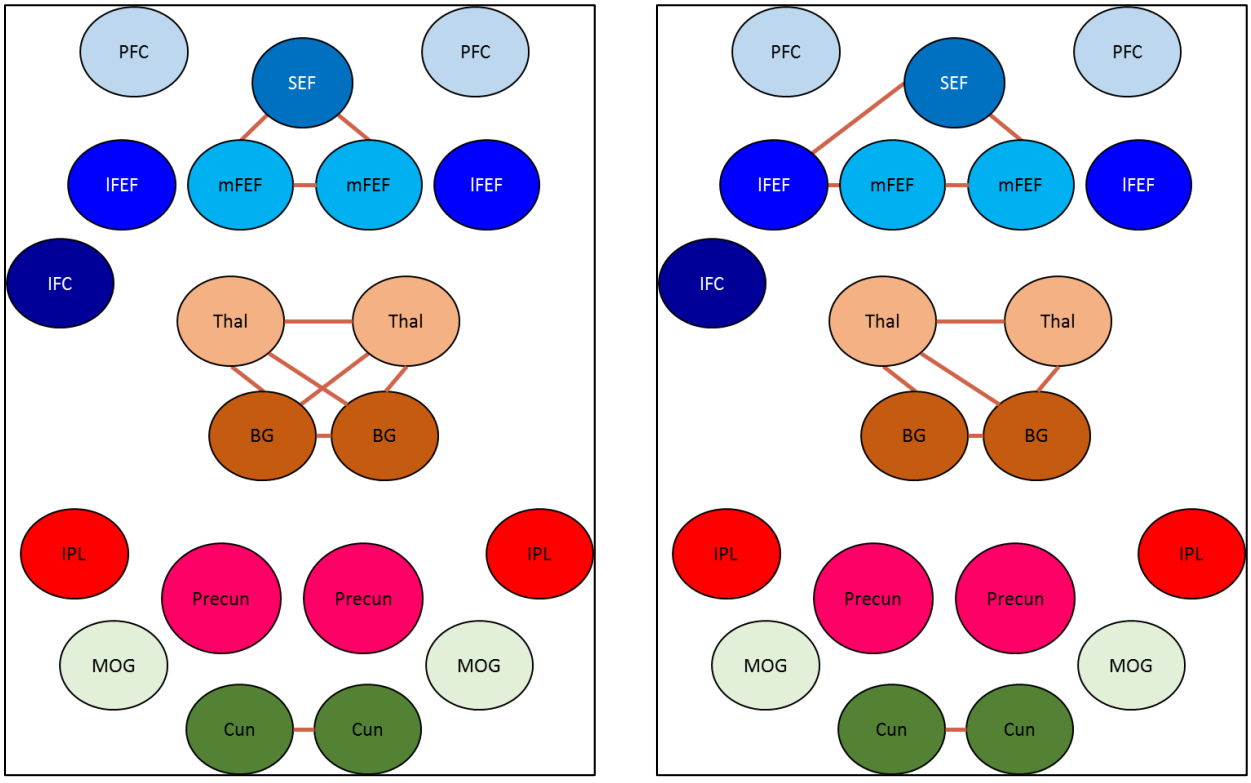

Figure 5.4 Specific practice group at pre-test (Left) and post-test (Right) for 100% event

Table 5.5 General practice group for 50% event

Strength of Connection	ROI connected	
	Pre-test	Post-test
1	lmedFEF – rmedFEF	lThal – rThal
2	lCun – rCun	lBG – rBG
3	lThal – rThal	lCun – rCun
4	lBG – rBG	rBG – rThal
5	rBG – rThal	lBG – lThal
6	lBG – lThal	lmedFEF – rmedFEF
7	lThal – rBG	lBG – rThal
8	rmedFEF – SEF	lThal – rBG
9	lmedFEF – SEF	rlatFEF – rmedFEF
10	lCun – rmedFEF	lCun – rlatFEF

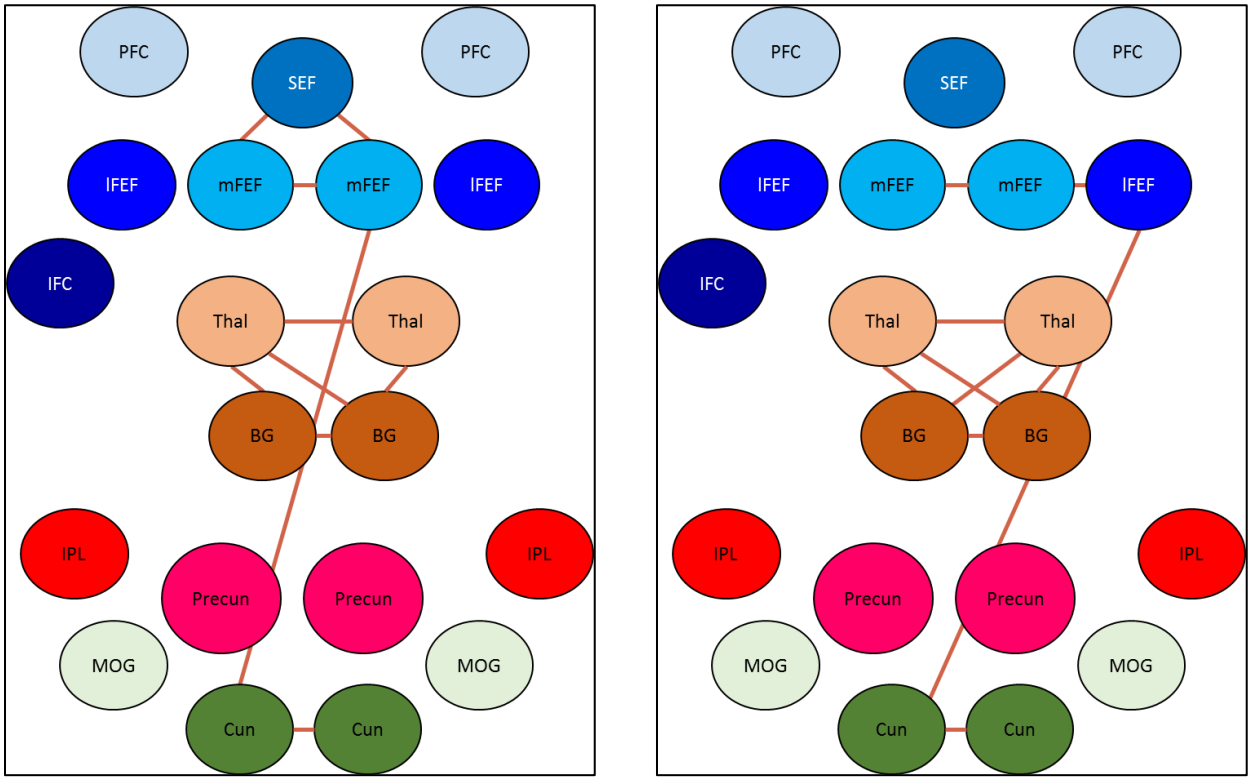

Figure 5.5 General practice group at pre-test (Left) and post-test (Right) for 50% event

Table 5.6 Specific practice group for 50% event

Strength of Connection	ROI connected	
	Pre-test	Post-test
1	lCun – rCun	lCun – rCun
2	lBG – rBG	lThal – rThal
3	lmedFEF – rmedFEF	lmedFEF – rmedFEF
4	lThal – rThal	rBG – rThal
5	lBG – lThal	lBG – rBG
6	rBG – rThal	rmedFEF – SEF
7	rmedFEF – SEF	lmedFEF – SEF
8	lThal – rBG	llatFEF – lmedFEF
9	lmedFEF – SEF	lThal – rBG
10	lBG – rThal	lBG – lThal

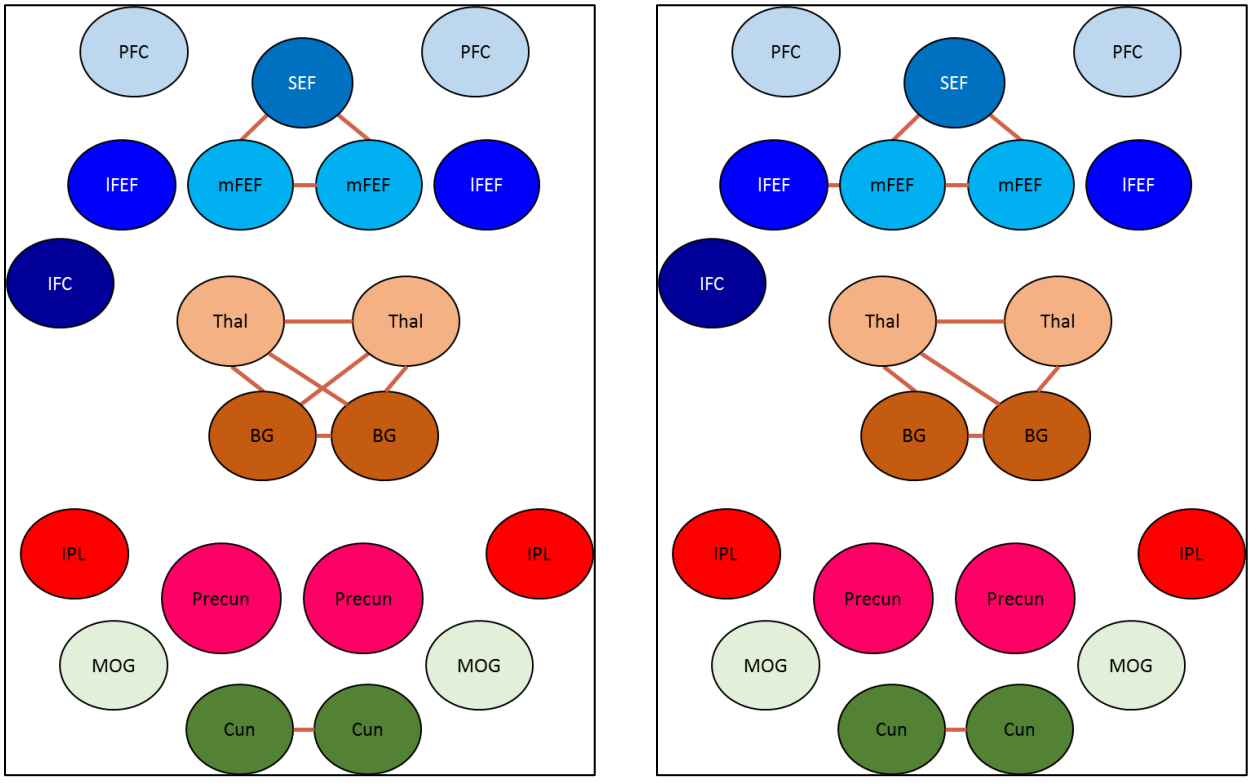

Figure 5.6 Specific practice group at pre-test (Left) and post-test (Right) for 50% event

Table 5.7 General practice group for blocked-design

Strength of Connection	ROI connected	
	Pre-test	Post-test
1	lmedFEF – rmedFEF	lmedFEF – rmedFEF
2	lCun – rCun	lCun – rCun
3	lThal – rThal	lBG – rBG
4	lBG – rBG	lThal – rThal
5	rBG – rThal	rBG – rThal
6	llatFEF – lmedFEF	lBG – lThal
7	lCun – lmedFEF	lmedFEF – SEF
8	lThal – rBG	llatFEF – lmedFEF
9	lmedFEF – lPrecun	lBG – rThal
10	rBG – rIPL	rmedFEF – SEF

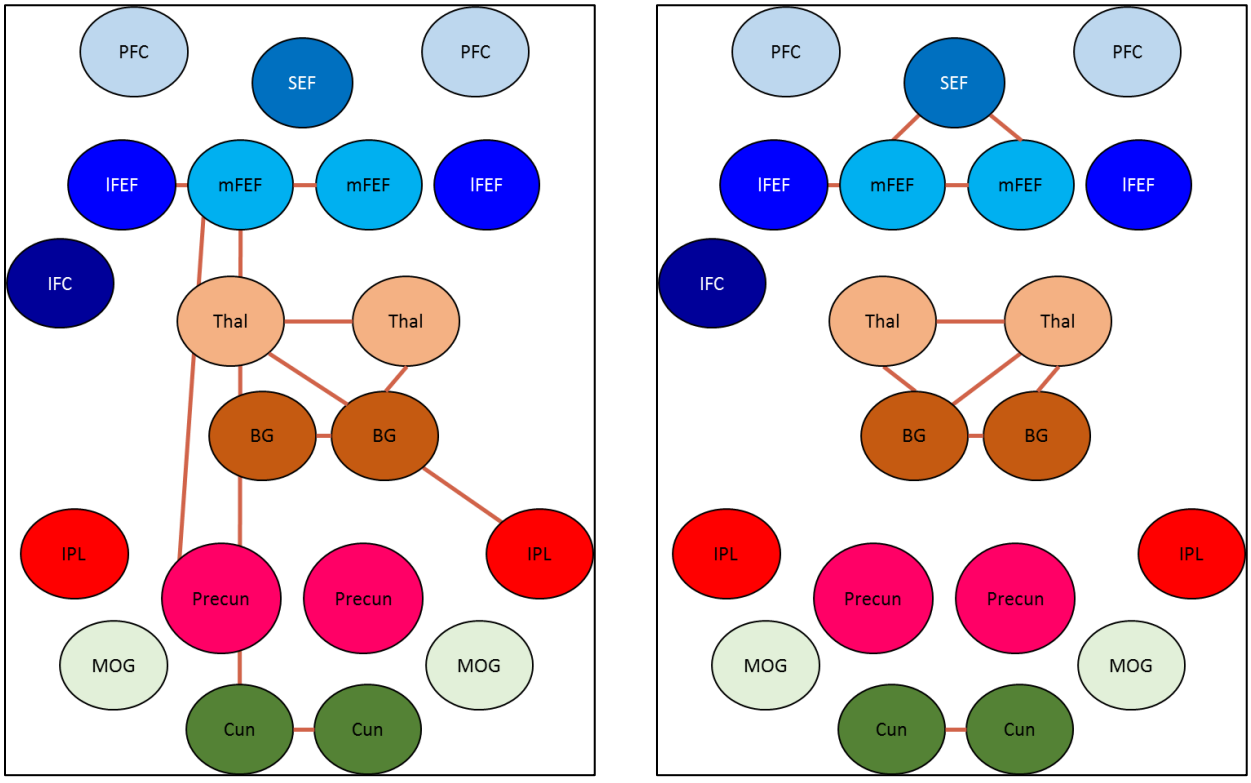

Figure 5.7 General practice group at pre-test (Left) and post-test (Right) for blocked-design

Table 5.8 Specific practice group for blocked-design

Strength of Connection	ROI connected	
	Pre-test	Post-test
1	lCun – rCun	lCun – rCun
2	lmedFEF – rmedFEF	lmedFEF – rmedFEF
3	lBG – rBG	lBG – rBG
4	lThal – rThal	lThal – rThal
5	rBG – rThal	llatFEF – rlatFEF
6	lmedFEF – SEF	llatFEF – rmedFEF
7	rmedFEF – SEF	rBG – rThal
8	lBG – lThal	llatFEF – lmedFEF
9	llatFEF – rlatFEF	lmedFEF – SEF
10	lThal – rBG	rlatFEF – rmedFEF

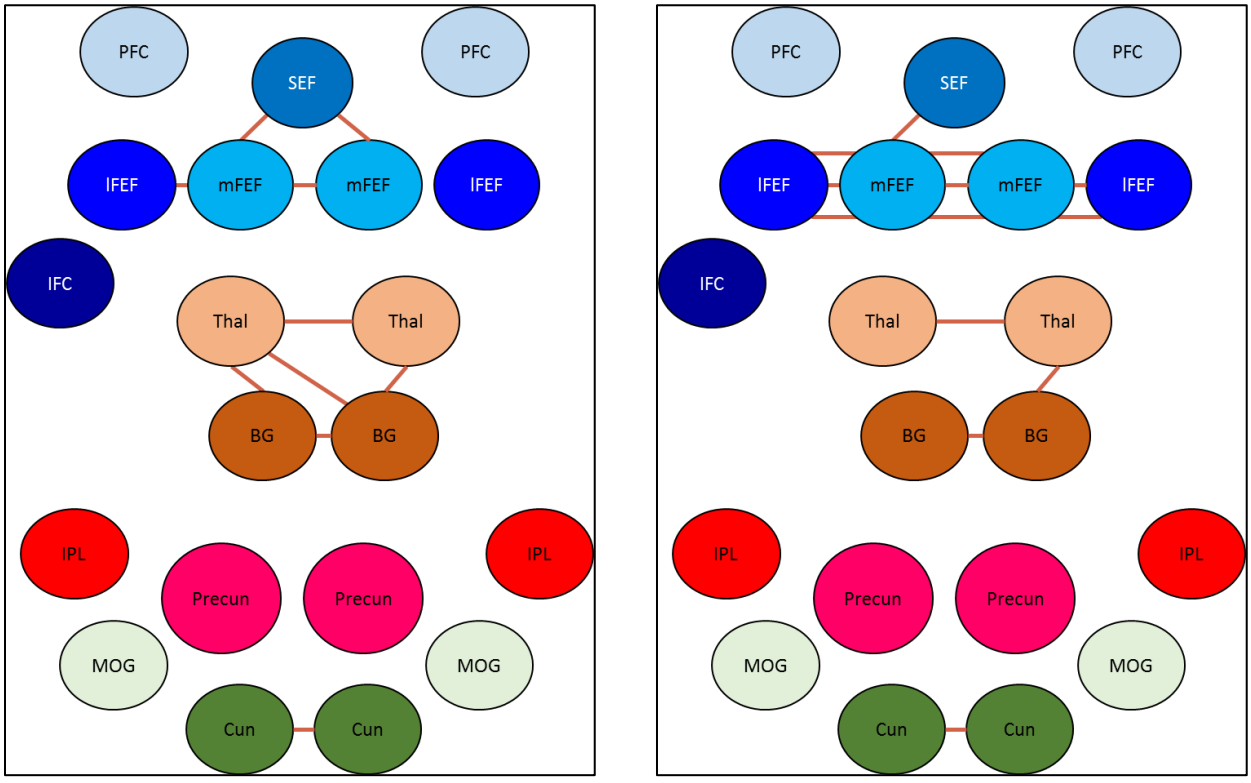

Figure 5.8 Specific practice group at pre-test (Left) and post-test (Right) for blocked-design

5.2 OVERALL RESULTS

To conduct a proper analysis on this fMRI data, we must examine it in different sections. We will begin by listing the strongest connections that appeared with the most frequency throughout all of the event datasets in Table 5.9. We will compare the results from the datasets that had the individuals participating in drastically different ratios of the saccadic eye movement tasks. Therefore we will be paralleling the 0% event with the 100% event and the 50% event with the blocked-design. Following these comparisons we will examine how frequently these connections appeared across the general and specific groups for pre and post-test in Table 5.10.

Recall that the 0% events did not include any antisaccade trials and the 100% events did not have any prosaccade trials. The general group practiced antisaccade trials while the specific group practiced both antisaccade and prosaccade trials. In general, they share the common connections such as Cun, Thal, BG and FEF as can be seen in Tables 5.1-5.4 and Figures 5.1-5.4. We note that FEF appeared more strongly in the 100% event than in the 0% event. The lBG – rThal appeared in the 0% general group and did not appear at all in the specific group. Similarly, the lmedFEF – SEF and rmedFEF – SEF connections only appeared in the specific group for the 0% and 100% events. One subtle difference between the two events is that lmedFEF – SEF appears in the 0% event three times opposed to one time in the 100% event. This subtle difference was not enough to alter the notion that these two groups are far more alike than dissimilar when it comes to their strongest connections.

When comparing the 50% event and blocked-design, we found it hard to find the practice effect through the graphs. The 50% event specific practice group did not appear to change very much from pre to post-test. However, the 50% event general practice group had the FEF – SEF connection in the pre-test, but was gone in the post-test. This is the exact opposite case for the

blocked-design general practice group. In the blocked-design post-test, we note that the FEF had more connections in the specific group than the general group. The specific blocked-design post-test group lost an FEF – SEF connection and lacked a lot of the BG – Thal connections that many other groups had. On the other hand we notice that llatFEF – lmedFEF appears in the blocked-design three times opposed to only once in the 50% event groups.

Table 5.9 Most Frequent Connections by Event

Strongest ROI Connections	Events			
	0%	100%	50%	Blocked-design
lCun – rCun	4	4	4	4
lThal – rThal	4	4	4	4
lBG – rBG	4	4	4	4
lmedFEF – rmedFEF	4	4	4	4
rBG – rThal	4	4	4	4
lThal – rBG	4	4	4	2
lBG – lThal	3	4	4	2
lBG – rThal	2	2	2	1
lmedFEF – SEF	3	1	3	3
rmedFEF – SEF	2	2	3	2

The numbers on the inside of Table 5.9 indicate the number of times that a connection appeared throughout the four events. The maximum this number can be is four because each event has two groups (general and specific) and two tests (pre and post). As clearly shown, the top five connections, in Table 5.9, appear in every dataset and the bottom five connections appear with less frequency but still seem relatively consistent across the events. In Table 5.10 we analyze the same ten connections, but look at them across the different groups instead of events.

Table 5.10 Most Frequent Connections by Group

Strongest ROI Connections	General		Specific	
	Pre	Post	Pre	Post
lCun – rCun	4	4	4	4
lThal – rThal	4	4	4	4
lBG – rBG	4	4	4	4
lmedFEF – rmedFEF	4	4	4	4
rBG – rThal	4	4	4	4
lThal – rBG	4	3	3	3
lBG – lThal	3	4	4	2
lBG – rThal	2	3	2	0
lmedFEF – SEF	1	2	4	3
rmedFEF – SEF	1	1	4	3

In Table 5.10, we see the most frequent connections separated by group instead of event as in Table 5.9. Notice that lBG – rThal, appears at least twice in every section besides the specific post-test group where it fails to appear at all. The lmedFEF – SEF and rmedFEF – SEF both appear over twice as many times in the specific groups than the general groups. These were the three connections that really stood apart from the others across the general and specific groups.

5.3 INDIVIDUAL TEST RESULTS

In the analysis done thus far, we have examined 16 datasets that represented the average of the subjects in each group. In future studies we would like to look at how individuals performed instead of the average of the individuals in each group. In Table 5.11 - Table 5.18 and Figure 5.9 – Figure5.16, we have begun to look at individual performance for the general practice group at pre-test for blocked-design. The tables and figures are recorded there from the 16 datasets, one dataset per subject.

In the following tables and plots you will quickly realize the diversity from subject to subject. For instance subjects 5, 7, 8, 9, 11, and 12 all seemed to activate the strongest connections across their whole brain instead of smaller areas. Subjects 2, 6, 9, and 11 had strong connections featuring IPL, which only appeared once in the averages section above. Other ROI that made appearance in the individuals, but not the averages were PFC and IFC. Conversely some ROI seemed to appear throughout like BG, Thal, Cun and mFEF, which follows what we learned in the section above with the averages.

In future studies, we would like to examine the individuals in all of the groups and compare them instead of just one group. This will give us a multitude of ways to dissect the datasets and gather insights about how the brain responds to these different saccade tests. It will also add to the diversity we see below as we transition from one subject to another.

Table 5.11 General practice group at pre-test for blocked-design with subjects 1-2

Strength of Connection	ROI connected	
	Subject 1	Subject 2
1	lBG – rBG	lThal – rThal
2	lCun – rCun	lBG – lThal
3	lmedFEF – rmedFEF	lBG - rBG
4	lBG – lThal	lCun – rCun
5	lThal – rThal	rBG – rThal
6	rBG – rThal	rCun – rMOG
7	lThal – rBG	lThal – rBG
8	lBG – rThal	lmedFEF – rmedFEF
9	llatFEF – SEF	lBG – rThal
10	lmedFEF – SEF	lIPL - rIPL

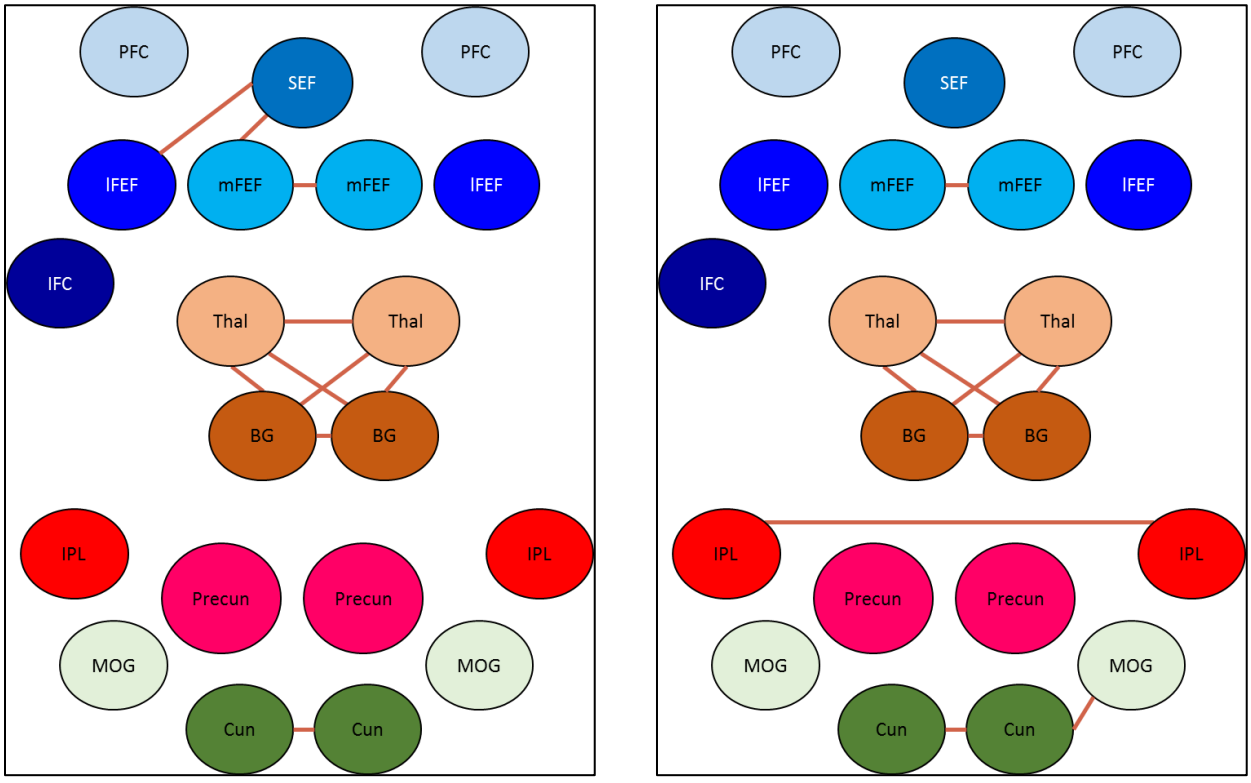

Figure 5.9 General practice group at pre-test for blocked-design with subjects 1-2 (left to right)

Table 5.12 General practice group at pre-test for blocked-design with subjects 3-4

Strength of Connection	ROI connected	
	Subject 3	Subject 4
1	lCun – rCun	lThal – rThal
2	lmedFEF – SEF	rBG – rThal
3	lmedFEF – rmedFEF	lBG – lThal
4	lThal – rThal	lBG – rBG
5	rBG – rThal	lBG – rThal
6	lBG - rBG	rmedFEF – SEF
7	llatFEF – lmedFEF	lmedFEF – rmedFEF
8	llatFEF – SEF	lThal – rBG
9	rmedFEF – SEF	lThal – rmedFEF
10	rPFC – SEF	IFC – SEF

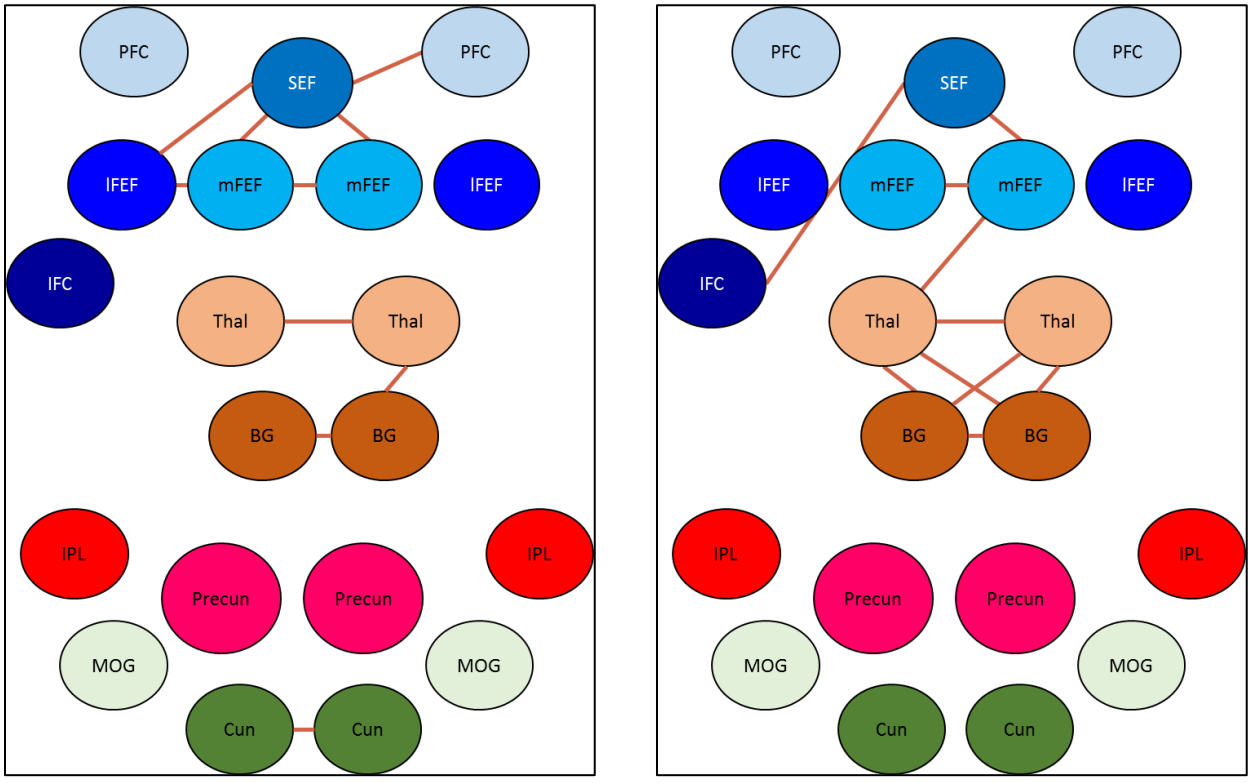

Figure 5.10 General practice group at pre-test for blocked-design with subjects 3-4 (left to right)

Table 5.13 General practice group at pre-test for blocked-design with subjects 5-6

Strength of Connection	ROI connected	
	Subject 5	Subject 6
1	lThal – rThal	lCun – rCun
2	lBG – rBG	lThal - rThal
3	lCun – rCun	lBG – rBG
4	lmedFEF – rmedFEF	rBG – rThal
5	rBG – rThal	lmedFEF – SEF
6	rCun – SEF	lBG – lThal
7	lMOG – rMOG	lThal – rBG
8	lBG – lThal	lIPL – rIPL
9	lBG – rThal	lBG – rThal
10	lThal – rBG	lmedFEF - rmedFEF

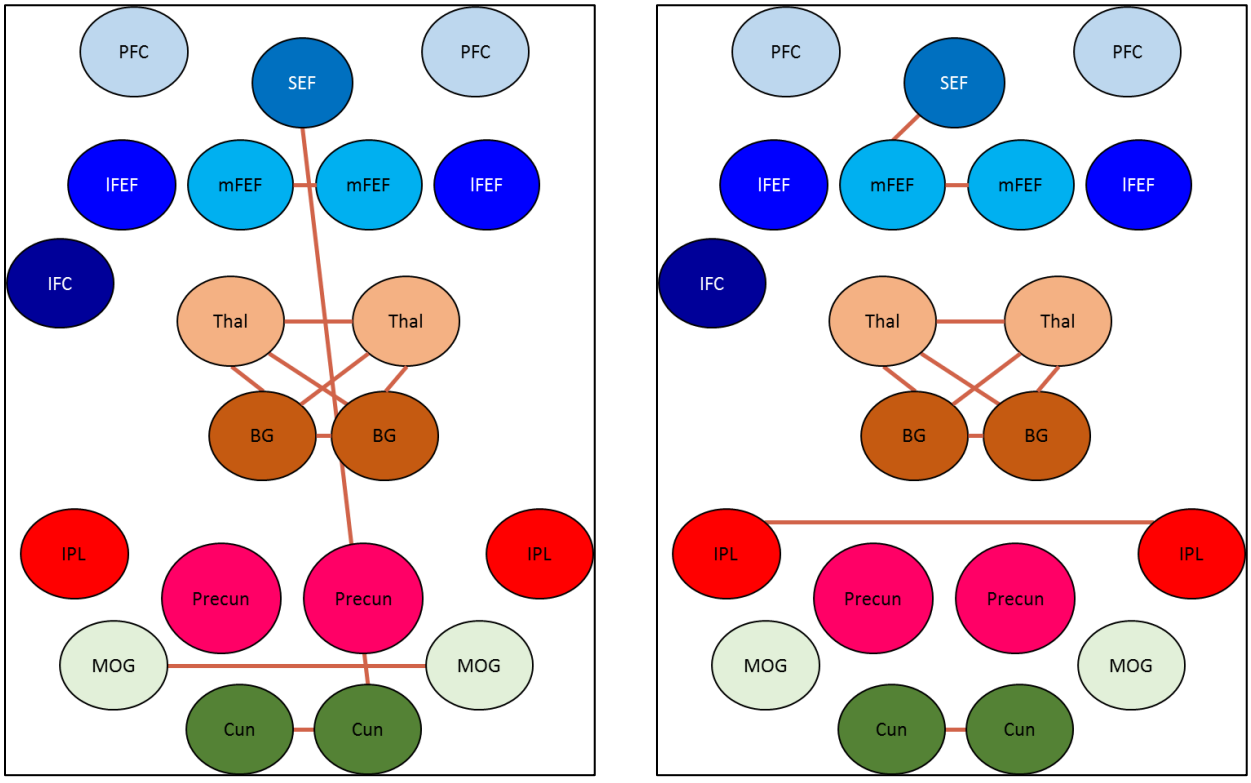

Figure 5.11 General practice group at pre-test for blocked-design with subjects 5-6 (left to right)

Table 5.14 General practice group at pre-test for blocked-design with subjects 7-8

Strength of Connection	ROI connected	
	Subject 7	Subject 8
1	lmedFEF – rmedFEF	lBG – rBG
2	lCun – rCun	lBG – lThal
3	rmedFEF – SEF	rBG – rThal
4	lBG – rBG	lCun – rCun
5	lThal – rThal	lmedFEF – rmedFEF
6	lmedFEF – SEF	lThal – rThal
7	rPrecun – SEF	lBG – rThal
8	rBG – rThal	lThal – rBG
9	lMOG – rMOG	rCun – rmedFEF
10	lCun – rPrecun	rmedFEF - rPrecun

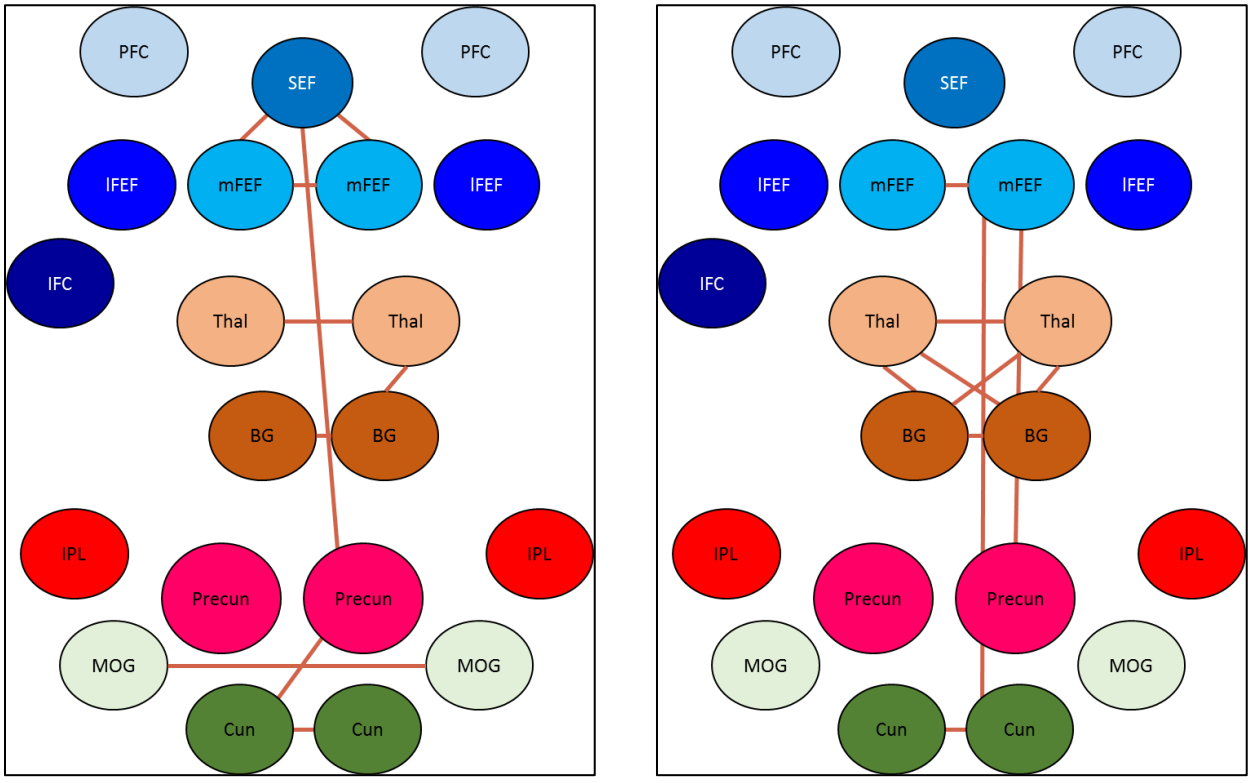

Figure 5.12 General practice group at pre-test for blocked-design with subjects 7-8 (left to right)

Table 5.15 General practice group at pre-test for blocked-design with subjects 9-10

Strength of Connection	ROI connected	
	Subject 9	Subject 10
1	lCun – rCun	lCun – rCun
2	lThal – rThal	lBG – rBG
3	lmedFEF – rmedFEF	lThal – rThal
4	lIPL – rIPL	lmedFEF – rmedFEF
5	lBG – rBG	rmedFEF – SEF
6	rIPL – SEF	rBG – rThal
7	lIPL – SEF	lmedFEF – SEF
8	rBG – rThal	lBG – lThal
9	lThal – rBG	lBG – rThal
10	lmedFEF – SEF	lThal – rBG

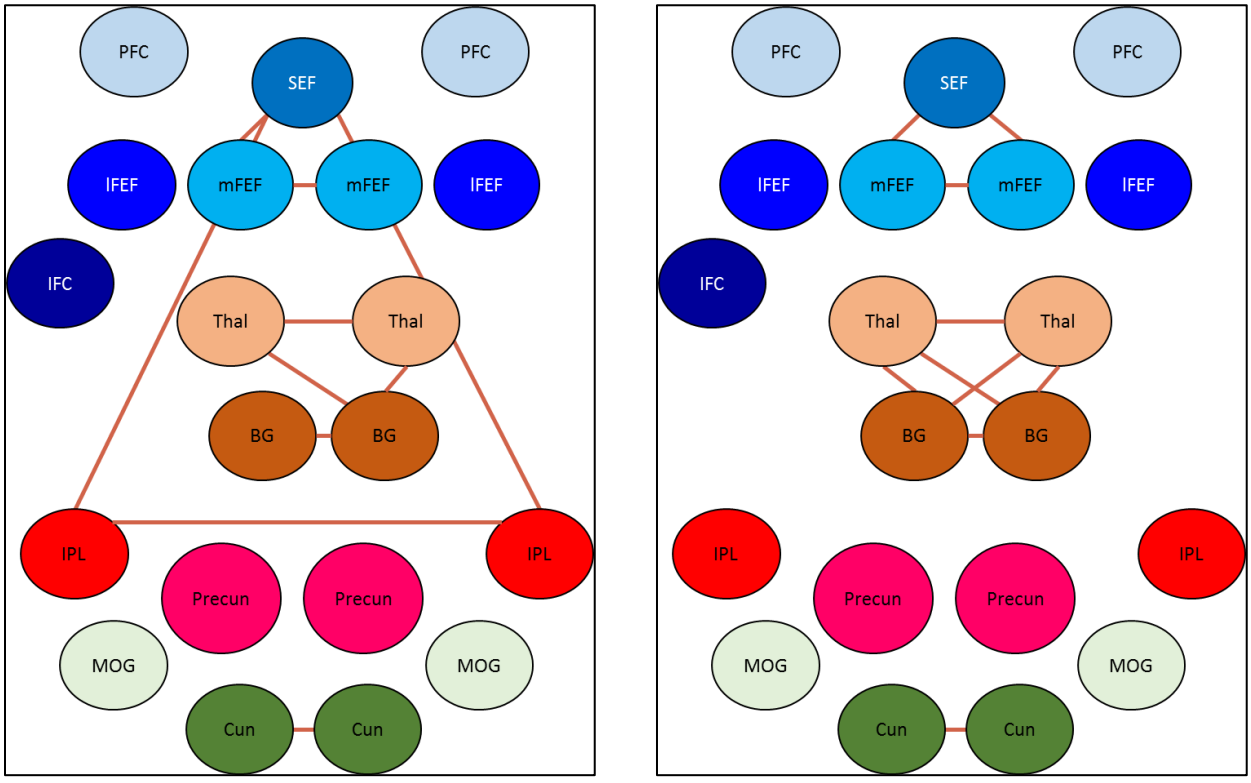

Figure 5.13 General practice group at pre-test for blocked-design with subjects 9-10

(left to right)

Table 5.16 General practice group at pre-test for blocked-design with subjects 11-12

Strength of Connection	ROI connected	
	Subject 11	Subject 12
1	lBG – rBG	lThal – rThal
2	lmedFEF – rmedFEF	lBG – rBG
3	lThal – rBG	lCun – rCun
4	lBG – lThal	lmedFEF – rmedFEF
5	lIPL – rIPL	rBG - rThal
6	llatFEF – SEF	lThal – rBG
7	lThal – rThal	lMOG – rMOG
8	rBG - rThal	lmedFEF - rPrecun
9	lCun - rmedFEF	lPFC – rmedFEF
10	lIPL - IFC	rmedFEF - rPrecun

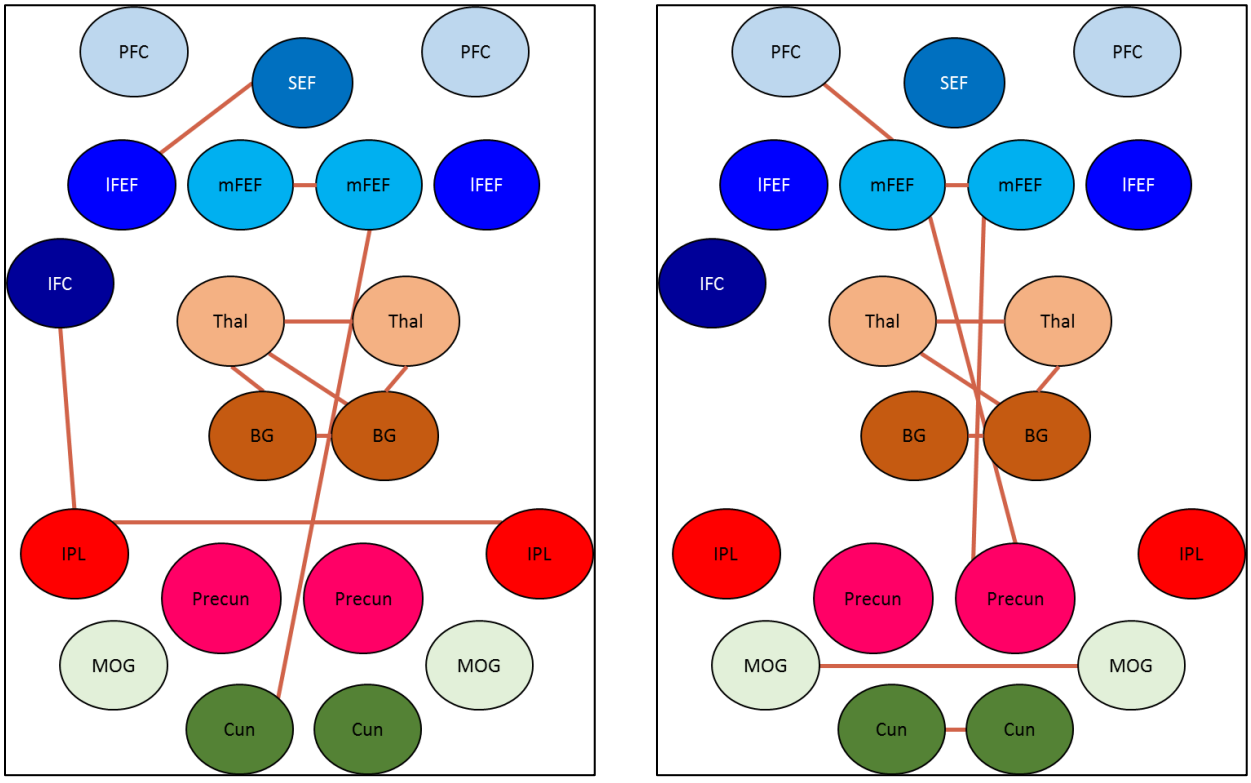

Figure 5.14 General practice group at pre-test for blocked-design with subjects 11-12

(left to right)

Table 5.17 General practice group at pre-test for blocked-design with subjects 13-14

Strength of Connection	ROI connected	
	Subject 13	Subject 14
1	lBG – rBG	lThal – rThal
2	lThal – rThal	lBG – rBG
3	lBG – lThal	lCun – rCun
4	lCun – rCun	lmedFEF – rmedFEF
5	lmedFEF – rmedFEF	lmedFEF – SEF
6	rBG – rThal	rmedFEF – SEF
7	lBG – rThal	rThal – SEF
8	lThal – rBG	rBG – rThal
9	lmedFEF – SEF	lThal – SEF
10	rmedFEF – SEF	lThal – rBG

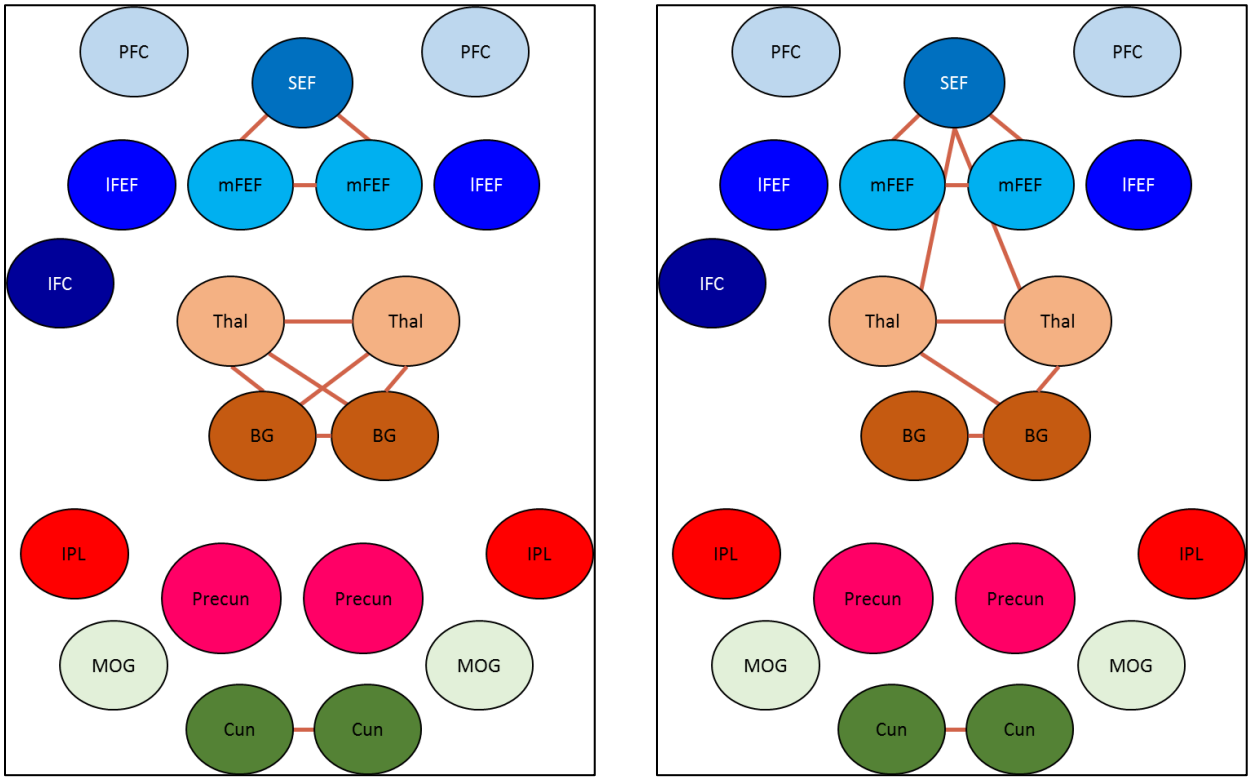

Figure 5.15 General practice group at pre-test for blocked-design with subjects 13-14

(left to right)

Table 5.18 General practice group at pre-test for blocked-design with subject 15-16

Strength of Connection	ROI connected	
	Subject 15	Subject 16
1	lCun – rCun	lThal – rThal
2	lBG – rBG	lBG – rBG
3	lmedFEF – rmedFEF	lmedFEF – rmedFEF
4	rBG – rThal	lThal – rBG
5	lBG – rThal	rBG – rThal
6	lThal – rThal	lBG – lThal
7	lBG – lThal	lmedFEF – SEF
8	rPrecun – SEF	rmedFEF – SEF
9	lThal – rBG	lThal – SEF
10	lMOG – rMOG	lBG – rThal

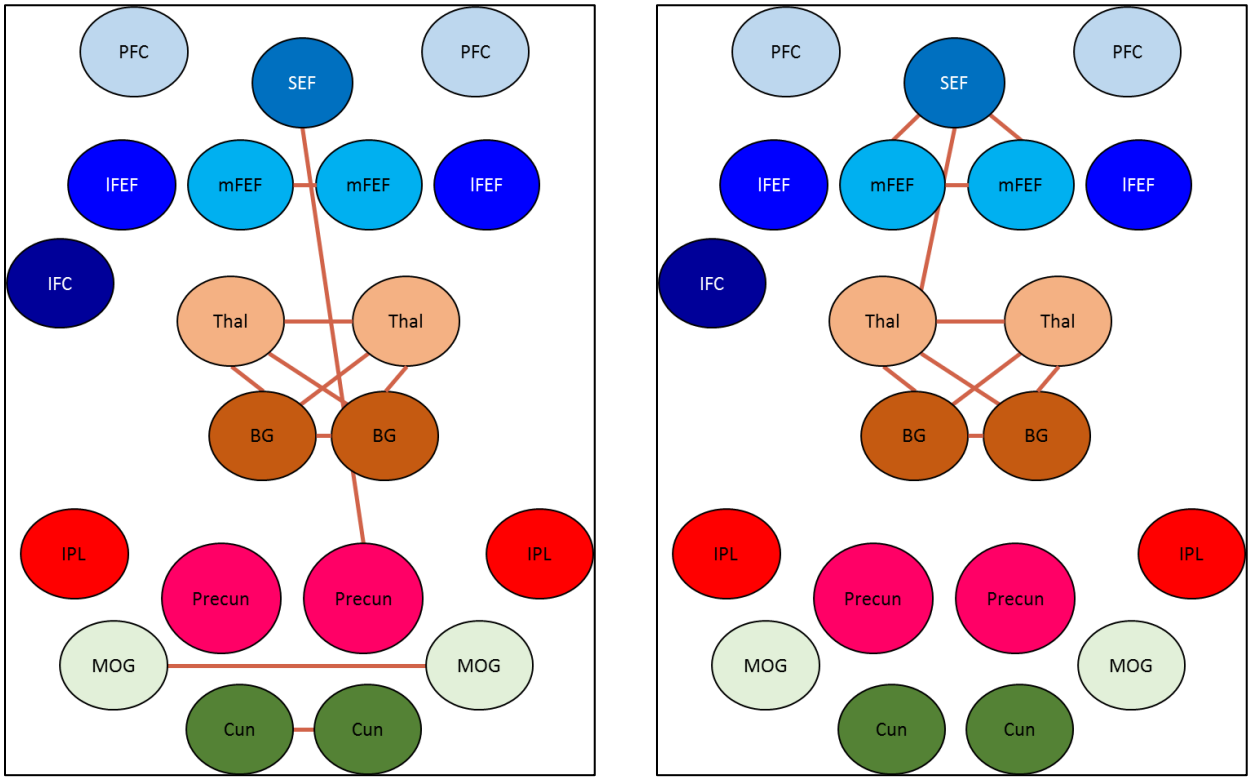

Figure 5.16 General practice group at pre-test for blocked-design with subjects 15-16

(left to right)

CHAPTER 6

CONCLUSION

In this thesis we evaluated brain activation using the graphical lasso procedure. We were also able to derive graphical representations of the fMRI data. We figured out which ROI had the strongest relationships, pre and post-test in all three event groups and the blocked-design group. We were also able to generate useful code for future work using the graphical lasso procedure.

In all methods it is very important to note the limitations that may exist and provide caution, before any action is implemented based on the results of the analysis. In this case the limitations are that data are observed sequentially, which can cause auto-correlation. This procedure treats each time as independent of others, but they are not because of the factor just mentioned. This is a subject that we could potentially investigate in any future work that we may conduct on this project.

In the current analysis, we examined 32 datasets that represented the average of the subjects in each group. In the future we would like to examine more than the top ten strongest connections in each group. We would also like to look at how more individuals (in all the groups) performed instead of the average of the individuals in each group. This will give us some different ways of looking at the data and seeing how diverse the human brain is from person to person.

REFERENCES

[1] Friedman, Jerome, Trevor Hastie, and Robert Tibshirani (2010a), "A Note on the Group Lasso and a Sparse Group Lasso." *ArXiv e-prints*, 1001.0736.

[2] Friedman, Jerome, Trevor Hastie, and Robert Tibshirani (2010b), "Applications of the Lasso and Grouped Lasso to the Estimation of Sparse Graphical Models." http://statweb.stanford.edu/~tibs/ftp/ggraph.pdf

[3] Koller, Daphne, and Nir Friedman (2012), *Probabilistic Graphical Models Principles and Techniques*. Cambridge, Mass.: MIT

[4] Lee, Jinae, Cheolwoo Park, Kara A. Dyckman, Nicole A. Lazar, Benjamin P. Austin, Qingyang Li, and Jennifer E. Mcdowell (2013), "Practice-related Changes in Neural Activation Patterns Investigated via Wavelet-based Clustering Analysis." *Human Brain* Mapping, 34, 2276-291.

[5] Luo, Xi (2014), "A Hierarchical Graphical Model for Big Inverse Covariance Estimation with an Application to FMRI." *ArXiv e-prints*, 1403.4698.

[6] Meinshausen, Nicolai and Bühlmann, Peter (2006), "High Dimensional Graphs and Variable Selection with the Lasso." *Annals of Statistics*, 34, 1436–1462.

[7] Pierce, Jordan E., and Jennifer E. Mcdowell (2017), "Reduced Cognitive Control Demands after Practice of Saccade Tasks in a Trial Type Probability Manipulation." *Journal of Cognitive Neuroscience*, 29, 368-81.

[8] Tibshirani, Robert (1996) “Regression Shrinkage and Selection via the Lasso.” *Journal of the Royal Statistical Society: Series B*, 58, 267-88.

[9] Wright, Stephen J (2015) “Coordinate Descent Algorithms.” *Mathematical Programming*, 151, 3-34.

[10] Yuan, Ming, and Yi Lin (2007) “Model Selection and Estimation in the Gaussian Graphical Model.” *Biometrika* 94, 19-35.

[11] Zhao, Tuo, Han Liu, Kathryn Roeder, John Lafferty, and Larry Wasserman, (2012) “The Huge Package for High-dimensional Undirected Graph Estimation in R.” *The Journal of Machine Learning Research* 13, 1059-062.